

Next-to-leading power endpoint factorization and resummation for off-diagonal “gluon” thrust

M. Beneke,^{a,b} M. Garny,^a S. Jaskiewicz,^c J. Strohm,^{a,b} R. Szafron,^d L. Vernazza^{e,f} and J. Wang^g

^a*Physik Department T31, Technische Universität München, James-Frank-Straße 1, D-85748 Garching, Germany*

^b*Excellence Cluster ORIGINS, Technische Universität München, D-85748 Garching, Germany*

^c*Institute for Particle Physics Phenomenology, Durham University, South Road, Durham, DH1 3LE, U.K.*

^d*Department of Physics, Brookhaven National Laboratory, Upton, NY 11973, U.S.A.*

^e*INFN, Sezione di Torino, Via P. Giuria 1, I-10125 Torino, Italy*

^f*Nikhef, Science Park 105, NL-1098 XG Amsterdam, The Netherlands*

^g*School of Physics, Shandong University, Shandan 27, Jinan, China*

E-mail: mathias.garny@tum.de, sebastian.jaskiewicz@durham.ac.uk, julian.strohm@tum.de, rszafron@bnl.gov, leonardo.vernazza@to.infn.it, j.wang@sdu.edu.cn

ABSTRACT: The lack of convergence of the convolution integrals appearing in next-to-leading-power (NLP) factorization theorems prevents the applications of existing methods to resum power-suppressed large logarithmic corrections in collider physics. We consider thrust distribution in the two-jet region for the flavour-nonsinglet off-diagonal contribution, where a gluon-initiated jet recoils against a quark-antiquark pair, which is power-suppressed. With the help of operatorial endpoint factorization conditions, we obtain a factorization formula, where the individual terms are free from endpoint divergences in convolutions and can be expressed in terms of renormalized hard, soft and collinear functions in four dimensions. This allows us to perform the first resummation of the endpoint-divergent SCET_I observables at the leading logarithmic accuracy using exclusively renormalization-group methods. The presented approach relies on universal properties of the soft and collinear limits and may serve as a paradigm for the systematic NLP resummation for other $1 \rightarrow 2$ and $2 \rightarrow 1$ collider physics processes.

KEYWORDS: Effective Field Theories of QCD, Factorization, Renormalization Group, Resummation

ARXIV EPRINT: [2205.04479](https://arxiv.org/abs/2205.04479)

Contents

| | | |
|----------|--|-----------|
| 1 | Introduction | 1 |
| 2 | Heuristic discussion | 3 |
| 3 | Bare factorization theorem | 5 |
| 3.1 | A-type term (soft quark) | 7 |
| 3.2 | B-type term | 10 |
| 3.3 | Tree-level evaluation | 14 |
| 4 | Endpoint factorization | 15 |
| 4.1 | Soft-collinear limit of the B1 matching coefficients | 16 |
| 4.2 | Endpoint factorization consistency conditions | 18 |
| 4.3 | Endpoint factorization formula | 20 |
| 5 | Renormalization-group equations | 24 |
| 5.1 | RGEs for the A-type functions | 24 |
| 5.2 | RGEs for the B-type functions | 27 |
| 6 | Resummation | 30 |
| 6.1 | Counting of logarithms and proper choice of scales | 31 |
| 6.2 | Double-logarithmic limit | 34 |
| 6.3 | Leading logarithms and running coupling effects | 35 |
| 7 | Conclusion | 38 |
| A | C^{B1} and D^{B1} | 40 |
| A.1 | One-loop results | 40 |
| A.2 | Derivation of the evolution equation of the asymptotic refactorization coefficient D^{B1} | 41 |
| B | Alternative version of the endpoint-finite factorization formula | 45 |

1 Introduction

Hadronic event shape variables in the two-jet region have played a key role for the development of resummation techniques in QCD [1, 2].¹ Later, the utility of soft-collinear effective theory (SCET) in extending the resummation order beyond what was achieved

¹See [3–6] for other early work discussing the break-down of the expansion in the strong coupling for back-to-back jets and semi-inclusive particle production.

with diagrammatic methods has first been demonstrated for the thrust variable T [7]. In the present work we develop the factorization of thrust for the particular contribution to the two-jet region, when a gluon recoils (at leading order) against a quark-antiquark pair (“gluon thrust”). The motivation for this derives from the fact that this process is of next-to-leading power (NLP) in $1 - T \ll 1$ in the two-jet region, and thus not covered by the existing factorization theorem. It represents the hadronic e^+e^- annihilation analogue of the off-diagonal qg parton channels in deep-inelastic scattering (DIS) at large Bjorken- x , or in Drell-Yan (DY) production near threshold. These and the power corrections to the corresponding diagonal channels have recently received much attention [8–20] in an effort to extend the classical leading-power (LP) factorization theorems for these observables to NLP in the kinematic regime, where large logarithms spoil the weak-coupling expansion. We focus on gluon thrust here, since it presents the same difficulties as the forementioned off-diagonal processes, but does not require the factorization of parton distribution functions.

The thrust of a hadronic event in e^+e^- annihilation with center-of-mass energy Q is defined as

$$T = \max_{\vec{n}} \frac{\sum_i |\vec{p}_i \cdot \vec{n}|}{\sum_i |\vec{p}_i|}, \tag{1.1}$$

where i runs over all hadrons (partons) in the final state. The plane orthogonal to the thrust axis \vec{n} divides space into a left and right hemisphere. The total invariant mass (squared) of the hadrons in these hemispheres will be denoted by M_L^2 and M_R^2 , respectively. As

$$\tau = 1 - T \rightarrow 0, \tag{1.2}$$

the particles cluster into a pair of back-to-back jets, and perturbation theory in the strong coupling $\alpha_s(Q)$ breaks down due to large logarithms $\ln \tau$ at every order. This has been extensively studied for the leading quark-antiquark two-jet process. All-order resummations are essential to provide reliable calculations of thrust and jet masses in the two-jet regions. In this work we consider instead the phase-space region

$$e^+e^- \rightarrow \gamma^* \rightarrow [g]_c + [q\bar{q}]_{\bar{c}}, \tag{1.3}$$

where the direction of gluon jet is defined to be the “collinear direction” and the direction of the recoiling $q\bar{q}$ -jet the “anti-collinear” one. This process starts at order α_s only (see figure 1). More importantly, as $\tau \rightarrow 0$, it does not have the leading-power $[\ln \tau / \tau]_+$ behaviour from soft-gluon emission. Instead the leading term is $\alpha_s \ln \tau$, and the entire process is of next-to-leading power in τ ,² similar to the off-diagonal DIS and DY processes related by crossing.

“Gluon thrust” and its unconventional all-order logarithmic structure was first studied in [14] and an expression for the leading double logarithms was written down, which was subsequently derived from d -dimensional consistency relations [18]. The result of [14] exhibits an unconventional “quark” Sudakov form factor, related to an enhancement when

²For clarification, we note that we do not consider here non-perturbative power corrections in the strong interaction scale Λ_{QCD} , which are expected to be $\mathcal{O}(\Lambda_{\text{QCD}}/(\tau Q))$, that is, we assume the strong hierarchy $\Lambda_{\text{QCD}}/Q \ll \tau \ll 1$.

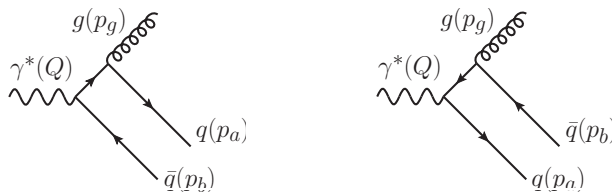


Figure 1. Leading $\mathcal{O}(\alpha_s)$ QCD diagrams contributing to gluon thrust.

either the quark or anti-quark in the $q\bar{q}$ -jet becomes soft. In this case the octet colour charge of the gluon jet is balanced by anti-collinear particles in a colour-triplet or anti-triplet. The colour mismatch of the back-to-back energetic particles causes a new type of double logarithms proportional to the difference $C_A - C_F$ of the colour charges at the leading double-logarithmic order. Despite these insights, and sketches of the form of a factorization theorem within SCET [11, 14, 18], it is not yet known how to proceed beyond the double-logarithmic order. The issue is an endpoint-divergence in the convolution integrals that link the hard, (anti-) collinear and soft functions in the factorization theorem. In the present work we build on refactorization ideas developed for DIS [18], and Higgs decay to two photons through bottom-quark loops [21, 22] to derive a factorization theorem suitable for systematic resummation. To this end we combine standard SCET factorization with endpoint factorization.

The outline of this paper is as follows: in section 2 we provide a heuristic discussion of the factorization formula, which motivates the proposed endpoint subtraction. In section 3 we derive the “bare” factorization theorem using standard SCET methods. For endpoint factorization to work, the hard, collinear and soft functions must satisfy certain asymptotic conditions, which are derived in section 4, and subsequently employed to rearrange the factorization formula such that the convolution integrals are finite. The renormalization-group equations required for the various functions are given in section 5 and solved with leading-logarithmic (LL) accuracy. Finally, in section 6, we obtain the resummed gluon thrust distribution and display the numerical effect of resummation.

Throughout the paper, we employ dimensional regularization with $d = 4 - 2\epsilon$ space-time dimensions, and the $\overline{\text{MS}}$ subtraction scheme whenever renormalization is required.

2 Heuristic discussion

At leading order (LO) a virtual photon couples to a quark-antiquark pair producing two back-to-back jets in the center-of-mass frame. In this work, we consider instead the different two-jet situation, where one of the jets is initiated by a gluon. This process is not only suppressed by one power of α_s (see figure 1) relative to the LO process, but also by one power of τ .

We define the hemisphere of the gluon jet to be in the “collinear” direction, the other jet is then in the “anti-collinear” direction. There are two possibilities to generate the gluon jet at $\mathcal{O}(\alpha_s)$:

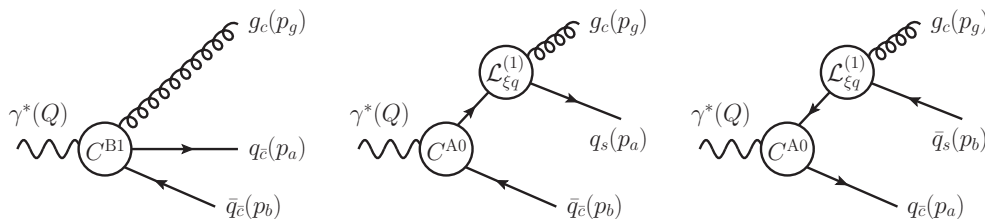


Figure 2. SCET representation of the “off-diagonal” gluon-thrust amplitude in the two-jet region. The diagrams show the NLP structure of the process with all LP interactions removed.

- I Quark and anti-quark have both large anti-collinear momentum and form a single jet, which recoils against the gluon.
- II The quark or anti-quark is anti-collinear and balances the gluon momentum, while the other of the two is soft.

Both configurations are suppressed by a factor of τ . Their further evolution is determined by the standard leading-power collinear splittings and soft emissions. The above separation introduces an ambiguity from the precise meaning of “soft” and “anti-collinear”. We can start with situation I, and decrease the large anti-collinear momentum component of the quark or anti-quark. At some point, it becomes soft (and anti-collinear) and should be counted as part of contribution II. In perturbative computations in powers of α_s , this ambiguity is not a problem as long as the jet definition is infrared-safe. If, however, one wants to perform resummation, the effective field theory approach requires the separation of soft and collinear modes to split the large logarithms into single-scale quantities. This conflict between physical and mathematical mode separation leads to a so-called endpoint divergence in the convolution integrals appearing in the factorization theorems.

Let us analyze these two possibilities from the SCET point of view by looking first at the Feynman diagrams shown in figure 1. We begin with I (later called “B-type” contribution, following the SCET notation for the corresponding hard vertex). The intermediate propagator in the diagram on the left carries momentum $q_a = p_g + p_a$. Since p_g is assumed to be collinear and p_a is anti-collinear, q_a is a hard momentum with virtuality $q_a^2 \sim Q^2$. The q_a -internal line is integrated out, and the primary hard SCET vertex produces a $q\bar{q}g$ state directly, see the first diagram in figure 2. Since there are two partons ($q\bar{q}$) in the anti-collinear direction, only their total momentum is fixed and the amplitude depends on the fraction of anti-collinear momentum carried by each parton. When one of these fractions tends to zero, the parton becomes effectively soft and one moves to possibility II (called “A-type” later). The q_a -internal line (or q_b , if the anti-quark becomes soft) is no longer hard. Hence the primary vertex is the standard $\gamma^* \rightarrow q\bar{q}$ process. The energetic quark or anti-quark subsequently transfers its entire momentum to the gluon, while becoming soft. This process is represented by a power-suppressed SCET Lagrangian term $\mathcal{L}_{\xi q}^{(1)}$ describing soft (anti-) quark emission, see the second and third diagrams in figure 2.

The fact that in some intermediate region the same physical process can be represented by the limits of two different mathematical expressions is the key to the idea of endpoint

factorization. To anticipate what will be discussed in technical terms further below, we state the factorization theorem for the two-hemisphere invariant mass distribution of gluon thrust in schematic form in Laplace space:

$$\begin{aligned} \frac{1}{\sigma_0} \frac{\widetilde{d\sigma}}{ds_R ds_L} &= \int_0^\Lambda d\omega d\omega' |C^{A0}|^2 \times \mathcal{J}_c^{(\bar{q})} \times \mathcal{J}_c(\omega, \omega') \otimes S_{\text{NLP}}(\omega, \omega') \\ &+ \int_{\Lambda/Q}^{1-\Lambda/Q} dr dr' C^{B1}(r) C^{B1}(r')^* \otimes \mathcal{J}_c^{q\bar{q}}(r, r') \times \mathcal{J}_c^{(g)} \times S^{(g)}. \end{aligned} \quad (2.1)$$

Here C are hard matching coefficients, \mathcal{J} are jet functions and S are soft functions. The precise definitions will be given in subsequent sections. We dropped all function arguments except for the convolution variables, which have divergent integrals. The soft-collinear ω, ω' convolution integrals are logarithmically divergent for $\omega, \omega' \rightarrow \infty$, while the hard-anti-collinear integrals over r, r' diverge logarithmically when $r, r' \rightarrow 0, 1$. However, both integrals are well-defined in dimensional regularization as long as the limit to four space-time dimensions is not taken.

In the intermediate region, the soft quark in the soft function S_{NLP} that appears in possibility II has *large* soft momentum ω and can equally well be regarded as part of the anti-collinear function $\mathcal{J}_c^{q\bar{q}}$ in the second line with *small* anti-collinear momentum fraction r . Removing the quark from S_{NLP} leaves the single-particle soft function $S^{(g)}$, hence $S_{\text{NLP}} \rightarrow S^{(g)}$ and $\mathcal{J}_c^{(\bar{q})} \rightarrow \mathcal{J}_c^{q\bar{q}}$. At the same time, the hard process changes from A0-type to B1-type. Thus, the *integrand*s of the two terms in (2.1) should become identical in the respective limits. A rearrangement at the integrand level can then be performed in the singular limits, which introduces the factorization parameter Λ , such that both integrals are separately finite. At this point one can remove the dimensional regulator and use standard renormalization-group techniques to sum the logarithms in the hard, jet and soft functions. These involve only LP interactions. NLP interactions occur only once (at amplitude level), leading to the two terms in (2.1), and therefore provide only one additional logarithmic, but finite integration from the convolutions.

3 Bare factorization theorem

The distribution of an event shape e in e^+e^- annihilation into hadrons through a photon with virtuality $Q^2 = q^2$ is

$$\frac{d\sigma}{de} = \sum_X \int d\text{PS}_X (2\pi)^d \delta^{(d)}(q - p_X) L_{\mu\nu}(q) \delta(e - \hat{e}(X)) \langle 0 | J^{\dagger\nu}(0) | X \rangle \langle X | J^\mu(0) | 0 \rangle, \quad (3.1)$$

with the leptonic tensor

$$L_{\mu\nu}(q) = \frac{8\pi^2 \alpha_{\text{em}}^2}{3Q^4} \left(-g_{\mu\nu} + \frac{q_\mu q_\nu}{Q^2} \right) \quad (3.2)$$

and the electromagnetic current $J^\mu = \bar{\psi} \gamma^\mu \psi$, for simplicity of a single quark flavour with electric charge $e_\psi = +1$. For a given final state X , $\hat{e}(X)$ returns the value of the event shape variable. For small τ ,

$$\tau = \frac{M_R^2 + M_L^2}{Q^2} + \mathcal{O}(\tau^2), \quad (3.3)$$

and the thrust distribution is related to the two-hemisphere invariant-mass distribution by

$$\frac{d\sigma}{d\tau} = \int dM_R^2 dM_L^2 \delta\left(\tau - \frac{M_R^2 + M_L^2}{Q^2}\right) \frac{d\sigma}{dM_R^2 dM_L^2}. \quad (3.4)$$

Eq. (3.1) is the starting point of the perturbative computation in terms of partonic final states X . The LP factorization theorem for the resummed event shape in the two-jet limit has been known for a long time [1, 2]. The resummation of NLP double-logarithmic corrections to the quark-antiquark back-to-back jet configuration, which is present already at LP, has been derived recently [9]. Defining the left hemisphere to be the collinear one and employing the SCET framework, the hemisphere invariant-mass distribution for $M_R^2, M_L^2 \ll Q^2$ is expressed at LP as

$$\frac{1}{\sigma_0} \frac{d\sigma}{dM_R^2 dM_L^2} = |C^{A0}(Q^2)|^2 \int dl_+ dl_- \mathcal{J}_c^{(q)}(M_L^2 - Ql_-) \mathcal{J}_{\bar{c}}^{(\bar{q})}(M_R^2 - Ql_+) S_{LP}(l_+, l_-) \quad (3.5)$$

in terms of the convolution of the jet (anti-) collinear functions with the hemisphere-soft function, multiplied by a universal hard function [7, 23–25].³ The distribution is normalized to the leading-order total cross section

$$\sigma_0 = \frac{4\pi N_c \alpha_{\text{em}}^2}{3Q^2}, \quad (3.6)$$

with the number of colours $N_c = 3$. Factorization theorems at NLP are more complicated due to multi-local convolutions, which further exhibit endpoint divergences, when expressed in terms of renormalized hard, collinear and soft functions [15].

Before turning to endpoint factorization, we provide in this section the SCET derivation of the factorization formula for off-diagonal gluon thrust, which has already been outlined in [14]. We introduce two light-like vectors n_{\pm}^{μ} , satisfying $n_+ n_- = 2$ and pointing into the directions of the back-to-back jets. The vector n_-^{μ} defines the direction of the collinear modes of the gluon jet. (Anti-) collinear modes therefore have large components $n_+ p_c \sim Q$ ($n_- p_{\bar{c}} \sim Q$). The transverse momenta in the jet are of order $p_{\perp} \sim \lambda Q \sim \sqrt{\tau} Q \ll Q$, where $\lambda \sim \sqrt{\tau}$ denotes the SCET power-counting parameter. The momenta of soft particles scale uniformly, $p_s \sim \tau Q$. In the adopted reference frame, $q_{\perp}^{\mu} = 0$. We further note that since gluon thrust vanishes at LP, there are no kinematic NLP corrections, and (3.3), (3.4) continue to hold.

After integrating out the hard modes, the electromagnetic current matches to

$$\begin{aligned} \bar{\psi} \gamma_{\perp}^{\mu} \psi(0) &= \int dt d\bar{t} \tilde{C}^{A0}(t, \bar{t}) \bar{\chi}_c(tn_+) \gamma_{\perp}^{\mu} \chi_{\bar{c}}(\bar{t}n_-) + (c \leftrightarrow \bar{c}) \\ &+ \sum_{i=1,2} \int dt d\bar{t}_1 d\bar{t}_2 \tilde{C}_i^{\text{B1}}(t, \bar{t}_1, \bar{t}_2) \bar{\chi}_{\bar{c}}(\bar{t}_1 n_-) \Gamma_i^{\mu\nu} \mathcal{A}_{c\perp\nu}(tn_+) \chi_{\bar{c}}(\bar{t}_2 n_-) + \dots \end{aligned} \quad (3.7)$$

in SCET. Here $\mathcal{A}_{c\perp\nu}$ denotes the gauge-invariant gluon field operator dressed with Wilson lines, which in light-cone gauge is related to the gluon field by $\mathcal{A}_{c\perp\nu} = g_s A_{c\perp\nu}$. The omitted terms are higher than NLP corrections and purely gluonic “flavour-singlet” operators.

³By charge conjugation symmetry, the quark and anti-quark jet functions coincide, $\mathcal{J}_{\bar{c}}^{(\bar{q})}(p^2) = \mathcal{J}_c^{(q)}(p^2)$.

For simplicity, we neglect the mixing of $q\bar{q}$ into gg operators in the second line. Singlet terms cause well-understood technical complications but do not touch the essence of the factorization discussed in this work.

The originally local current is now represented by light-ray operators. The first line corresponds to the LP hard vertex, which emits a back-to-back quark-antiquark pair. The second line of (3.7) represents the $\mathcal{O}(\lambda)$ suppressed ‘‘B-type’’ SCET operator, which directly produces the configuration relevant to gluon thrust, a collinear gluon and an anti-collinear quark-antiquark pair. The first line can nevertheless contribute to gluon thrust through a time-ordered product with the $\mathcal{O}(\lambda)$ suppressed SCET interaction [26, 27]

$$\mathcal{L}_{\xi q}(x) = \bar{q}_s(x_-)\mathcal{A}_{c\perp}(x)\chi_c(x) + \text{h.c.}, \quad (3.8)$$

which converts a collinear quark into a collinear gluon and a soft quark. Here

$$x_{\mp}^{\mu} = (n_{\pm} \cdot x) \frac{n_{\mp}^{\mu}}{2}, \quad (3.9)$$

and we further define the scalar quantity $x_{\mp} \equiv n_{\pm} \cdot x/2$. The gluon jet now recoils against a quark-antiquark pair in a highly asymmetric configuration, in which the antiquark carries almost all the momentum of the jet.⁴ The Dirac structures in the power-suppressed B-type operator are given by

$$\Gamma_1^{\mu\nu} = \frac{\not{n}_-}{2} \gamma_{\perp}^{\nu} \gamma_{\perp}^{\mu}, \quad \Gamma_2^{\mu\nu} = \frac{\not{n}_-}{2} \gamma_{\perp}^{\mu} \gamma_{\perp}^{\nu}. \quad (3.10)$$

We note that boost invariance together with the projection property $\not{n}_-\chi_c = 0$, $\not{n}_+\chi_{\bar{c}} = 0$ implies that only the transverse components of the vector current contribute.

Eq. (3.7) is the starting point for deriving the factorization formula and the main steps are fairly standard. After the collinear field redefinition with the soft Wilson line [28] $Y_{n_-}(x) = \mathcal{P} \exp [ig_s \int_0^{\infty} ds n_- A_s(x + sn_-)]$ ($Y_{n_+}(x)$ for anti-collinear fields), the collinear, anti-collinear and soft fields are decoupled at LP. The final state $|X\rangle = |X_c\rangle|X_{\bar{c}}\rangle|X_s\rangle$ consists of a collection of corresponding modes, and hence the matrix element factorizes into suitably defined collinear, anti-collinear and soft functions. Performing these steps on the two terms in (3.7), more precisely the time-ordered product with (3.8) for the first, gives rise to an ‘‘A-type’’ and a ‘‘B-type’’ term in the factorization formula, which we discuss separately next. Note that due to the different field/mode content in the final state (soft quark or not), there is no interference between the two terms when squaring the amplitude.

3.1 A-type term (soft quark)

This term stems from the square of the matrix element

$$\langle X_c | \langle X_{\bar{c}} | \langle X_s | \int d^d x T [\bar{\chi}_c(tn_+) \gamma_{\perp}^{\mu} \chi_{\bar{c}}(\bar{t}n_-), i\mathcal{L}_{\xi q}(x)] | 0 \rangle, \quad (3.11)$$

summed and integrated over all possible final states. As mentioned above, there are two A-type terms, because either the quark or the anti-quark in the current can transfer its

⁴The hermitian conjugate in (3.8) provides a second contribution, in which the antiquark turns into the collinear gluon and a soft antiquark.

momentum to the collinear gluon. Due to the different final state, the two terms do not interfere. In (3.11) we consider explicitly only the first contribution. We comment on the second at the end. To separate the above matrix element into collinear, anti-collinear and soft factors, we perform the field redefinitions [28]

$$\chi_c(x) \rightarrow Y_{n_-}(x_-)\chi_c(x), \quad \chi_{\bar{c}}(x) \rightarrow Y_{n_+}(x_+)\chi_{\bar{c}}(x), \quad (3.12)$$

$$\mathcal{A}_{c\perp}^\mu(x) \rightarrow Y_{n_-}(x_-)\mathcal{A}_{c\perp}^\mu(x)Y_{n_-}^\dagger(x_-). \quad (3.13)$$

Inspection of (3.7), (3.11) shows that the following hard, (anti-) collinear and soft functions appear.

Hard function. This term involves the hard function $\tilde{C}^{\text{A0}}(t, \bar{t})$ of the LP A-type current. We define the momentum-space coefficient

$$C^{\text{A0}}(n_+p_c, n_-p_{\bar{c}}) = \int dt d\bar{t} e^{itn_+p_c + i\bar{t}n_-p_{\bar{c}}} \tilde{C}^{\text{A0}}(t, \bar{t}). \quad (3.14)$$

It depends only on the product $Q^2 = n_+p_c n_-p_{\bar{c}}$ of the large components of the collinear and anti-collinear momenta. At LO, we find $C^{\text{A0}}(Q^2) = 1 + \mathcal{O}(\alpha_s)$. The two-loop result can be found in [29].

Anti-collinear function. The \mathcal{L}_{ξ_q} Lagrangian insertion acts in the collinear sector, hence the anti-collinear sector is unaffected. After squaring the amplitude and integrating over the anti-collinear final state, we obtain the LP anti-quark jet function

$$\begin{aligned} & \frac{1}{2\pi} \sum_{X_{\bar{c}}} \int d\text{PS}_{X_{\bar{c}}} \langle 0 | \bar{\chi}_{\bar{c}}(x)_{b\beta} | X_{\bar{c}} \rangle \langle X_{\bar{c}} | \chi_{\bar{c}}(0)_{a\alpha} | 0 \rangle \\ & \equiv \delta_{ab} \int \frac{d^d p}{(2\pi)^d} n_- p e^{-ipx} \mathcal{J}_{\bar{c}}^{(\bar{q})}(p^2) \left(\frac{\not{p}_+}{2} \right)_{\alpha\beta}. \end{aligned} \quad (3.15)$$

At LO, we have $\mathcal{J}_{\bar{c}}^{(\bar{q})}(p^2) = \delta^+(p^2) \equiv \theta(p^0)\delta(p^2)$. This object is well understood and computed up to the third order in α_s [30]. Here and below we use small Latin letters for colour and Greek letters for Dirac spinor indices.

Collinear function. This function picks up the collinear fields from the \mathcal{L}_{ξ_q} insertion and represents a new non-local jet function that appears at NLP. Defining the non-local operator

$$\mathcal{O}_{a\alpha; b\beta}(\omega, x) = \int d^d y e^{iy-\omega} T \{ \bar{\chi}_{c, b\beta}(x), [\mathcal{A}_{\perp c} \chi_c]_{a\alpha}(x+y) \}, \quad (3.16)$$

where $y_- = n_+ \cdot y/2$, its jet function defined as in the LP case (3.15) by

$$\begin{aligned} & \frac{1}{2\pi} \sum_{X_c} \int d\text{PS}_{X_c} \frac{1}{g_s^2} \langle 0 | \mathcal{O}_{b'\beta'; a'\alpha'}^\dagger(\omega', x) | X_c \rangle \left[\frac{\not{p}_+}{2} \right]_{\alpha'\alpha} \langle X_c | \mathcal{O}_{a\alpha; b\beta}(\omega, 0) | 0 \rangle \\ & = (d-2) \left[\frac{\not{p}_-}{2} \right]_{\beta'\beta} \int \frac{d^d p}{(2\pi)^d} e^{-ipx} \left\{ [t^A]_{ab} [t^A]_{b'a'} \mathcal{J}_c(p^2, \omega, \omega') \right. \\ & \quad \left. + [t^A]_{aa'} [t^A]_{b'b} \hat{\mathcal{J}}_c(p^2, \omega, \omega') \right\}. \end{aligned} \quad (3.17)$$

The factor $1/g_s^2$ has been introduced for convenience, such that the leading term is $\mathcal{O}(\alpha_s^0)$. The Dirac matrix $[\not{\eta}_+/2]_{\alpha'\alpha}$ on the left-hand side ensures that only a single Dirac structure can appear on the right-hand side, and avoids a discussion of evanescent structures that would otherwise be present. In the derivation of the A-type term, this factor will arise from the decomposition of the soft function, see (3.20) below.⁵ At LO in α_s , the collinear final state X_c consists of a single gluon,⁶ and only the unhatted jet function is non-vanishing:

$$\mathcal{J}_c(p^2, \omega, \omega') = \frac{1}{\omega\omega'} \delta^+(p^2), \tag{3.18}$$

$$\widehat{\mathcal{J}}_c(p^2, \omega, \omega') = 0. \tag{3.19}$$

Soft function. Collecting the soft Wilson lines from the soft-decoupling field redefinition, as well as the soft quark field from the Lagrangian insertion (3.8) leads to the following definition of the NLP soft quark function:

$$\begin{aligned} & g_s^2 \int \frac{dx_-}{2\pi} \frac{dx'_-}{2\pi} e^{-i(x_- \omega - x'_- \omega')} \langle 0 | \bar{T} \left\{ \left[Y_{n_+}^\dagger(0) Y_{n_-}(0) \right]_{cb'} \left[Y_{n_-}^\dagger q_s \right]_{\alpha'a'}(x'_-) \right\} \\ & \times \mathcal{P}_s(l_+, l_-) T \left\{ \left[\bar{q}_s Y_{n_-} \right]_{\alpha a}(x_-) \left[Y_{n_-}^\dagger(0) Y_{n_+}(0) \right]_{bc} \right\} |0\rangle \\ & = \left(\frac{\not{\eta}_+}{2} \right)_{\alpha'\alpha} \left\{ \delta_{a'a} \delta_{bb'} S_{\text{NLP}}(l_+, l_-, \omega, \omega') + \delta_{ba} \delta_{a'b'} \widehat{S}_{\text{NLP}}(l_+, l_-, \omega, \omega') \right\} + \dots, \end{aligned} \tag{3.20}$$

where x_- is defined below (3.9), and

$$\mathcal{P}_s(l_+, l_-) \equiv \sum_{X_s} \int d\text{PS}_{X_s} \delta(l_+ - n_+ p_{X_s}^R) \delta(l_- - n_- p_{X_s}^L) |X_s\rangle \langle X_s|, \tag{3.21}$$

contains the measurement function on the soft final state and the final-state sum pertaining to the two-hemisphere invariant mass distribution. With this definition, the left hemisphere contains the collinear gluon jet, and the right hemisphere is on the anti-collinear side. The dots in (3.20) denote terms proportional to $\not{\eta}_-$, which do not contribute due to the projection property of collinear fields in other parts of the process. The prefactor is chosen for convenience, such that the soft function starts at $\mathcal{O}(\alpha_s)$. The soft function for thrust is obtained from

$$S_{\text{NLP}}^T(k, \omega, \omega') = \int_0^\infty dl_+ dl_- \delta(k - l_+ - l_-) S_{\text{NLP}}(l_+, l_-, \omega, \omega'). \tag{3.22}$$

There is an analogous definition with obvious modifications for the NLP soft anti-quark function relevant to the second A-type contribution. The colour decomposition is chosen such that at leading $\mathcal{O}(\alpha_s)$, $\widehat{S}_{\text{NLP}}(l_+, l_-, \omega, \omega') = 0$, while

$$\begin{aligned} S_{\text{NLP}}(l_+, l_-, \omega, \omega') = & \frac{\alpha_s}{4\pi} \frac{\theta(\omega) \delta(\omega - \omega')}{e^{-\epsilon\gamma_E} \Gamma(1 - \epsilon)} \left[\delta(l_-) \theta(\omega - l_+) \theta(l_+) \omega \left(\frac{l_+ \omega}{\mu^2} \right)^{-\epsilon} \right. \\ & \left. - \frac{\omega^2}{1 - \epsilon} \delta(l_+) \delta(l_- - \omega) \left(\frac{\omega^2}{\mu^2} \right)^{-\epsilon} \right]. \end{aligned} \tag{3.23}$$

⁵This would remain true even if we had allowed for flavour-singlet contractions of the quark fields. These do not exist for the A-type term, since the contraction of different modes, that is the collinear quark field with the soft quark field from the soft function, is not allowed in SCET.

⁶The $q\bar{q}g$ final state at this order corresponds to a disconnected diagram, which does not contribute to the scattering amplitude.

The two-hemisphere NLP soft-quark function is introduced here for the first time, but we take note of the calculation of the NLP soft function that appears for soft gluon emission in the Drell-Yan process [10], which is already known to $\mathcal{O}(\alpha_s^2)$ [10, 31].

Factorization formula. With these definitions, we obtain the soft-quark contribution to gluon thrust in the two-jet region in the form

$$\begin{aligned} \frac{1}{\sigma_0} \frac{d\sigma}{dM_R^2 dM_L^2} \Big|_{\text{A-type}} &= \frac{2C_F}{Q} f(\epsilon) |C^{A0}(Q^2)|^2 \int_0^\infty dl_+ dl_- \int d\omega d\omega' \mathcal{J}_{\bar{c}}^{(\bar{q})}(M_R^2 - Ql_+) \\ &\times \left\{ \mathcal{J}_c(M_L^2 - Ql_-, \omega, \omega') S_{\text{NLP}}(l_+, l_-, \omega, \omega') \right. \\ &\quad \left. + \widehat{\mathcal{J}}_c(M_L^2 - Ql_-, \omega, \omega') \widehat{S}_{\text{NLP}}(l_+, l_-, \omega, \omega') \right\}, \end{aligned} \quad (3.24)$$

where

$$f(\epsilon) = \left(\frac{Q^2}{4\pi} \right)^{-\epsilon} \frac{(1-\epsilon)^2 \Gamma(1-\epsilon)}{\Gamma(2-2\epsilon)} \quad (3.25)$$

is a d -dimensional factor defined such that $f(0) = 1$ in four dimensions.

To turn the convolution in l_+, l_- into a product, it is convenient to consider the Laplace transform

$$\frac{\widetilde{d\sigma}}{ds_R ds_L} = \int_0^\infty dM_R^2 dM_L^2 e^{-s_R M_R^2/Q} e^{-s_L M_L^2/Q} \frac{d\sigma}{dM_R^2 dM_L^2} \quad (3.26)$$

of the two-hemisphere invariant-mass distribution. In general, the Laplace transform of collinear functions with variable p^2 are defined with $\int_0^\infty dp^2 e^{-sp^2/Q}$, while for soft functions we use $\int_0^\infty dl_+ dl_- e^{-s_R l_+ - s_L l_-}$. Then

$$\begin{aligned} \frac{1}{\sigma_0} \frac{\widetilde{d\sigma}}{ds_R ds_L} \Big|_{\text{A-type}} &= \frac{2C_F}{Q} f(\epsilon) |C^{A0}(Q^2)|^2 \widetilde{\mathcal{J}}_{\bar{c}}^{(\bar{q})}(s_R) \int d\omega d\omega' \\ &\times \left\{ \widetilde{\mathcal{J}}_c(s_L, \omega, \omega') \widetilde{S}_{\text{NLP}}(s_R, s_L, \omega, \omega') + \widetilde{\widehat{\mathcal{J}}}_c(s_L, \omega, \omega') \widetilde{\widehat{S}}_{\text{NLP}}(s_R, s_L, \omega, \omega') \right\}. \end{aligned} \quad (3.27)$$

The total A-type term is twice the above (3.24), (3.27), since there is an equal contribution from the soft anti-quark phase-space region.

3.2 B-type term

The B-type term is obtained under the assumption that the intermediate propagator in figure 1 is hard, which leads to the B1 operator in the matching equation (3.7). We then need the square of the matrix elements

$$\langle X_c | \langle X_{\bar{c}} | \langle X_s | \bar{\chi}_{\bar{c}}(\bar{t}_1 n_-) \Gamma_i^{\mu\nu} \mathcal{A}_{c\perp\nu}(tn_+) \chi_{\bar{c}}(\bar{t}_2 n_-) | 0 \rangle, \quad (3.28)$$

summed and integrated over all possible final states. Inspection of (3.7), (3.28) shows that the following hard, (anti-) collinear and soft functions appear.

Hard function. There are two relevant operators, $i = 1, 2$, which differ by their Dirac structures (3.10). We introduce the Fourier transforms

$$C_i^{\text{B1}}(n_+p_c, rn_-p_{\bar{c}}, \bar{r}n_-p_{\bar{c}}) = n_-p_{\bar{c}} \int dt d\bar{t}_1 d\bar{t}_2 e^{itn_+p_c + i(\bar{t}_1 r + \bar{t}_2 \bar{r})n_-p_{\bar{c}}} \tilde{C}_i^{\text{B1}}(t, \bar{t}_1, \bar{t}_2) \quad (3.29)$$

of the corresponding hard functions. The B-type operators contain two fields (quark and anti-quark) in the same collinear direction. The momentum-space coefficient depends on the product $Q^2 = n_+p_c n_-p_{\bar{c}}$ of the large components of the collinear and total anti-collinear momentum, and r , which denotes the fraction of total anti-collinear momentum carried by the quark. Accordingly, $\bar{r} = 1 - r$ is the momentum fraction of the anti-quark. At the leading order in α_s , we find⁷

$$C_1^{\text{B1}}(Q^2, r) = \frac{1}{r}, \quad (3.30)$$

$$C_2^{\text{B1}}(Q^2, r) = -\frac{1}{\bar{r}}. \quad (3.31)$$

From the transformation of (3.7) under charge conjugation, we find that charge conjugation invariance implies that $C_2^{\text{B1}}(Q^2, r) = -C_1^{\text{B1}}(Q^2, \bar{r})$ to all orders in the strong coupling. We notice that the matching coefficient C_1^{B1} (C_2^{B1}) is singular in the limit $r \rightarrow 0$ ($r \rightarrow 1$), in which the quark (anti-quark) becomes soft. From this observation, we can already anticipate a relation to the A-type contributions.

Further insight can be obtained by a helicity consideration. To this end, we separate the electromagnetic current in (3.7) into a left- and right-handed piece by inserting $1 = P_L + P_R$. In four space-time dimensions we have⁸

$$\Gamma_1^{\mu\nu} P_L = g_L^{\mu\nu} \not{n}_- P_L, \quad (3.32)$$

$$\Gamma_2^{\mu\nu} P_L = g_R^{\mu\nu} \not{n}_- P_L, \quad (3.33)$$

$$\Gamma_1^{\mu\nu} P_R = g_R^{\mu\nu} \not{n}_- P_R, \quad (3.34)$$

$$\Gamma_2^{\mu\nu} P_R = g_L^{\mu\nu} \not{n}_- P_R, \quad (3.35)$$

where

$$g_{L/R}^{\mu\nu} = \frac{1}{2} \left(g_{\perp}^{\mu\nu} \pm \frac{i}{2} \epsilon^{\rho\sigma\mu\nu} n_{-\rho} n_{+\sigma} \right) \quad (3.36)$$

projects on the left (-1) / right ($+1$) helicity of the collinear gluon in the B1 operator (3.7). Since helicity is conserved and amplitudes with gluons of different helicity do not interfere (see (3.37) below), the virtual photon and gluon always have the same helicity. Focusing on the negative helicity case for definiteness, we conclude from (3.32)–(3.35) that the operator with Dirac structure $\Gamma_1^{\mu\nu}$ produces a left-handed out-going quark, while for $\Gamma_2^{\mu\nu}$ it is right-handed. It follows that the two operators cannot interfere in the non-singlet channel, where the $\bar{\chi}_{\bar{c}}(\bar{t}_1 n_-) \chi_{\bar{c}}(\bar{t}_2 n_-)$ fields in the operator in (3.7) cannot be contracted among themselves. This strictly holds only in four space-time dimensions. In other words, a non-singlet interference term must be “evanescent” and vanish as $\epsilon \rightarrow 0$.

⁷We recall that the definition of $\mathcal{A}_{c\perp}^\mu$ absorbs the factor g_s from the tree-level diagram.

⁸Convention: $\epsilon^{0123} = +1$.

The limit $r \rightarrow 0$ in the B1 matching coefficient implies that the momentum of the outgoing quark in the left diagram of figure 1 goes to zero, and the intermediate quark propagator goes on-shell. The helicity argument above implies that only $C_1^{\text{B1}}(Q^2, r)$ corresponding to $\Gamma_1^{\mu\nu}$ can be singular in this limit. For definiteness, consider again the case of the negative helicity gluon and virtual photon. The nearly on-shell intermediate propagator implies that the B1 operator factorizes into $\gamma^* \rightarrow q + \bar{q}$ and $q \rightarrow q + g$. As $r \rightarrow 0$ the outgoing quark in the latter process has zero momentum, and the incoming quark and outgoing gluon have the same large collinear momentum. Since g has negative helicity, the incoming quark must be left-handed, since a helicity change by 3/2 is not possible. By helicity conservation of the strong interaction, the final soft quark must then also be left-handed. As shown above, this singles out $\Gamma_1^{\mu\nu}$. The situation is reversed in the soft anti-quark limit $r \rightarrow 1$ and implies right-handedness, which singles out $\Gamma_2^{\mu\nu}$. We conclude that, to all orders in perturbation theory, only $C_1^{\text{B1}}(Q^2, r)$ ($C_2^{\text{B1}}(Q^2, r)$) can be singular in the endpoint $r \rightarrow 0$ ($r \rightarrow 1$).

Collinear function. The collinear function is simply the standard LP gluon jet function, defined as

$$\begin{aligned} \frac{1}{2\pi} \frac{1}{g_s^2} \sum_{X_c} \int d\text{PS}_{X_c} \langle 0 | \mathcal{A}_{c\perp\mu}^B(x) | X_c \rangle \langle X_c | \mathcal{A}_{c\perp\nu}^C(0) | 0 \rangle \\ \equiv \delta^{BC} (-g_{\mu\nu}^\perp) \int \frac{d^d p}{(2\pi)^d} e^{-ipx} \mathcal{J}_c^{(g)}(p^2). \end{aligned} \quad (3.37)$$

At LO, we have $\mathcal{J}_c^{(g)}(p^2) = \delta^+(p^2)$. This object is well understood and known up to the third order in α_s [32].

Anti-collinear function. The anti-collinear fields consist of the quark-anti-quark pair, which recoils against the gluon and is therefore in a colour-octet state. The corresponding jet function can be defined as for the gluon, but in terms of the composite field

$$\mathcal{Q}_i^{A\mu\nu}(x, r) = \frac{1}{2\pi} \int_0^\infty d\bar{t} e^{-ir\bar{t}n_- \cdot p_{\bar{c}}} \bar{\chi}_{\bar{c}}(x + \bar{t}n_-) t^A \Gamma_i^{\mu\nu} \chi_{\bar{c}}(x). \quad (3.38)$$

At leading order, r can be interpreted as the momentum fraction of the out-going quark. The Dirac structures refer to (3.10). Except for the colour and Dirac matrix, the operator coincides with the one that enters the definition of light-cone distribution amplitudes of mesons. However, instead of the vacuum-to-meson matrix element, here we need the inclusive jet function

$$\begin{aligned} \frac{g_s^2}{2\pi} \sum_{X_{\bar{c}}} \int d\text{PS}_{X_{\bar{c}}} \langle 0 | \mathcal{Q}_{i'\mu\nu}^{\dagger B}(x, r') | X_{\bar{c}} \rangle \langle X_{\bar{c}} | \mathcal{Q}_i^{A\mu\nu}(0, r) | 0 \rangle \\ = \delta^{AB} (d-2)^2 \int \frac{d^d p}{(2\pi)^d} e^{-ipx} \left\{ \delta_{ii'} \mathcal{J}_{\bar{c}}^{q\bar{q}(8)}(p^2, r, r') + (1 - \delta_{ii'}) \widehat{\mathcal{J}}_{\bar{c}}^{q\bar{q}(8)}(p^2, r, r') \right\}, \end{aligned} \quad (3.39)$$

which is a NLP object. It is easy to see that the four possible values of $i, i' = 1, 2$ give rise to only two independent jet functions, which we decompose as above into a diagonal

and off-diagonal term in ii' . At lowest non-vanishing order $\mathcal{O}(\alpha_s)$, the $X_{\bar{c}} = q\bar{q}$ final state results in

$$\mathcal{J}_{\bar{c}}^{q\bar{q}(8)}(p^2, r, r') = \frac{\alpha_s}{4\pi} \frac{1}{\Gamma(1-\epsilon)} \delta(r-r') r\bar{r} \left(\frac{\mu^2 e^{\gamma_E}}{p^2 r\bar{r}} \right)^\epsilon, \quad (3.40)$$

where $\bar{r} = 1 - r$.

The hatted function, which describes the interference of the two B1 operators, is given at this order by $\widehat{\mathcal{J}}_{\bar{c}}^{q\bar{q}(8)}(p^2, r, r') = (-\epsilon)/(1-\epsilon) \mathcal{J}_{\bar{c}}^{q\bar{q}(8)}(p^2, r, r')$, and vanishes in four dimensions, as expected from the helicity discussion above. In principle, it should be possible to remove this evanescent anti-collinear function by a finite, non-minimal counterterm related to its mixing into the “physical” jet function. This relies crucially on a renormalized factorization theorem, i.e. being able to take $\epsilon \rightarrow 0$ at the level of the individual collinear, soft etc. functions. Since for the time being, we continue to work with d -dimensional quantities, we keep $\widehat{\mathcal{J}}_{\bar{c}}^{q\bar{q}(8)}(p^2, r, r')$ in the following. We will see later that it is irrelevant for the discussion of endpoint divergences.

Soft function. Performing the soft decoupling field redefinition on (3.28) results in the field product

$$\bar{\chi}_{\bar{c}a}[Y_{n_+}^\dagger Y_{n_-}]_{ac}[t^B]_{cd}[Y_{n_-}^\dagger Y_{n_+}]_{db}\chi_{\bar{c}b}\mathcal{A}_{c\perp\nu}^B. \quad (3.41)$$

The Wilson lines can be combined into the adjoint Wilson lines \mathcal{Y}_{n_\mp} using

$$[Y_{n_\mp} t^A Y_{n_\mp}^\dagger]_{ab} = [Y_{n_\mp}^\dagger t^A Y_{n_\mp}]_{ab} = \mathcal{Y}_{n_\mp}^{AB}[t^B]_{ab}. \quad (3.42)$$

After squaring the matrix element and summing over the soft final state, we obtain the LP two-hemisphere soft function in the adjoint representation:

$$S^{(g)}(l_+, l_-) = \frac{1}{N_c^2 - 1} \langle 0 | \bar{T} \left\{ \mathcal{Y}_{n_+}^{BD}(0) \mathcal{Y}_{n_-}^{DA}(0) \right\} \mathcal{P}_s(l_+, l_-) T \left\{ \mathcal{Y}_{n_-}^{AC}(0) \mathcal{Y}_{n_+}^{CB}(0) \right\} | 0 \rangle. \quad (3.43)$$

The LO result is $S^{(g)}(l_+, l_-) = \delta(l_+) \delta(l_-)$.

Factorization formula. Inserting these matrix element definitions, we obtain the factorization formula for the B-type term

$$\begin{aligned} \frac{1}{\sigma_0} \frac{d\sigma}{dM_R^2 dM_L^2} \Big|_{\text{B-type}} &= \frac{2C_F}{Q^2} f(\epsilon) \int_0^\infty dl_+ dl_- \sum_{i,i'=1,2} \int dr dr' C_{i'}^{\text{B1}*}(Q^2, r') C_i^{\text{B1}}(Q^2, r) \\ &\times \left\{ \delta_{ii'} \mathcal{J}_{\bar{c}}^{q\bar{q}(8)}(M_R^2 - Ql_+, r, r') + (1 - \delta_{ii'}) \widehat{\mathcal{J}}_{\bar{c}}^{q\bar{q}(8)}(M_R^2 - Ql_+, r, r') \right\} \\ &\times \mathcal{J}_c^{(g)}(M_L^2 - Ql_-) S^{(g)}(l_+, l_-). \end{aligned} \quad (3.44)$$

In Laplace space:

$$\begin{aligned} \frac{1}{\sigma_0} \frac{\widetilde{d\sigma}}{ds_R ds_L} \Big|_{\text{B-type}} &= \frac{2C_F}{Q^2} f(\epsilon) \sum_{i,i'=1,2} \int dr dr' C_{i'}^{\text{B1}*}(Q^2, r') C_i^{\text{B1}}(Q^2, r) \\ &\times \left\{ \delta_{ii'} \widetilde{\mathcal{J}}_{\bar{c}}^{q\bar{q}(8)}(s_R, r, r') + (1 - \delta_{ii'}) \widetilde{\widehat{\mathcal{J}}}_{\bar{c}}^{q\bar{q}(8)}(s_R, r, r') \right\} \widetilde{\mathcal{J}}_c^{(g)}(s_L) \widetilde{S}^{(g)}(s_R, s_L). \end{aligned} \quad (3.45)$$

Only the first term in the curly brackets proportional to $\delta_{ii'}$ is non-vanishing at leading $\mathcal{O}(\alpha_s)$.⁹

3.3 Tree-level evaluation

Inserting tree-level results for all functions given above, the two terms in equations (3.24) and (3.44) reduce to the following expressions. The A-type soft-quark term is given by

$$\begin{aligned}
 \frac{1}{\sigma_0} \frac{d^2\sigma}{dM_R^2 dM_L^2} \Big|_{\text{A-type, tree}} &= \frac{2C_F}{Q} f(\epsilon) \int dl_+ dl_- \int d\omega d\omega' \delta^+(M_R^2 - Ql_+) \\
 &\times \frac{1}{\omega\omega'} \delta^+(M_L^2 - Ql_-) \frac{\alpha_s}{4\pi} \frac{\theta(\omega)\delta(\omega - \omega')}{e^{-\epsilon\gamma_E}\Gamma(1-\epsilon)} \left[\delta(l_-) \theta(\omega - l_+) \theta(l_+) \omega \left(\frac{l_+\omega}{\mu^2} \right)^{-\epsilon} \right. \\
 &\qquad \qquad \qquad \left. - \frac{\omega^2}{1-\epsilon} \delta(l_+) \delta(l_- - \omega) \left(\frac{\omega^2}{\mu^2} \right)^{-\epsilon} \right] \\
 &= \frac{\alpha_s}{4\pi} \frac{2C_F}{Q^2} \frac{f(\epsilon)}{e^{-\epsilon\gamma_E}\Gamma(1-\epsilon)} \left[\frac{1}{\epsilon} \delta^+(M_L^2) \left(\frac{(M_R^2)^2}{Q^2\mu^2} \right)^{-\epsilon} - \delta^+(M_R^2) \frac{1}{1-\epsilon} \left(\frac{(M_L^2)^2}{Q^2\mu^2} \right)^{-\epsilon} \right], \quad (3.46)
 \end{aligned}$$

where the pole in ϵ arises from the logarithmic divergence of the integral $\int_{l_+}^{\infty} d\omega/\omega$ for large values of the soft function variable. The total A-type contribution is twice the above after adding the soft-antiquark term. Similarly, the B-type term is given by

$$\begin{aligned}
 \frac{1}{\sigma_0} \frac{d^2\sigma}{dM_L^2 dM_R^2} \Big|_{\text{B-type, tree}} &= \frac{2C_F}{Q^2} f(\epsilon) \int dl_+ dl_- \int_0^1 dr dr' \delta^+(M_L^2 - Ql_-) \delta(l_+) \delta(l_-) \quad (3.47) \\
 &\times \left\{ \left(\frac{1}{r} \frac{1}{r'} + \frac{1}{\bar{r}} \frac{1}{\bar{r}'} \right) + \left(\frac{1}{r} \frac{1}{\bar{r}'} + \frac{1}{\bar{r}} \frac{1}{r'} \right) \frac{\epsilon}{1-\epsilon} \right\} \delta(r - r') \frac{\alpha_s}{4\pi} \frac{r\bar{r}}{\Gamma(1-\epsilon)} \left(\frac{(M_R^2 - Ql_+) r\bar{r}}{\mu^2 e^{\gamma_E}} \right)^{-\epsilon} \\
 &= \frac{\alpha_s}{4\pi} \frac{4C_F}{Q^2} f(\epsilon) \left\{ -\frac{1}{\epsilon} + \frac{\epsilon}{(1-\epsilon)^2} \right\} \delta^+(M_L^2) \left(\frac{M_R^2}{\mu^2 e^{\gamma_E}} \right)^{-\epsilon} \frac{\Gamma(2-\epsilon)}{\Gamma(2-2\epsilon)}.
 \end{aligned}$$

In this case, the singularity arises from a logarithmic divergence in the integral over the momentum fraction r as $r \rightarrow 0$ and $r \rightarrow 1$. Adding both terms and taking the limit $\epsilon \rightarrow 0$, we find

$$\frac{1}{\sigma_0} \frac{d^2\sigma}{dM_L^2 dM_R^2} = \frac{\alpha_s C_F}{\pi} \frac{1}{Q^2} \left\{ \delta^+(M_L^2) \left[\ln \frac{Q^2}{M_R^2} - 1 \right] - \delta^+(M_R^2) \right\}. \quad (3.48)$$

The poles cancel in the sum of both the A and B-type contributions in equations (3.46) and (3.47) (once we account for the soft-antiquark contribution to the A-type term) as it should be, as the off-diagonal gluon-thrust is infrared safe. After converting the two-hemisphere invariant mass distribution to the thrust distribution according to (3.4), we reproduce the coefficient $-\alpha_s C_F/\pi$ of the $\ln \tau$ term in [33].

The single logarithm arises from the dimensionally regulated convolution integrals, which are logarithmically divergent in $d = 4$. For resummation we would like to define renormalized hard, soft and (anti) collinear functions and take the limit $\epsilon \rightarrow 0$ before

⁹Since the *sum* of the A-type and B-type term are finite in the limit $\epsilon \rightarrow 0$, the common prefactor $f(\epsilon)$ could be set to its four-dimensional value 1 everywhere at this point.

performing the convolution integrals. Proceeding in this way, however, the convolution integrals are ill-defined. In the following sections we explain how this problem can be solved.

To prepare this discussion we make the following observation. The integrand of the two-dimensional convolution in ω, ω' in (3.46) in the limit of large ω, ω' (where the divergence arises) is given by

$$\begin{aligned} & \frac{\alpha_s}{4\pi} \frac{2C_F}{Q} f(\epsilon) \int dl_+ dl_- \delta^+(M_R^2 - Ql_+) \delta^+(M_L^2 - Ql_-) \delta(l_-) \theta(l_+) \\ & \times \frac{\delta(\omega - \omega')}{\omega\omega'} \frac{1}{e^{-\epsilon\gamma_E} \Gamma(1 - \epsilon)} \omega \left(\frac{l_+ \omega}{\mu^2} \right)^{-\epsilon} \\ & = \frac{\alpha_s}{4\pi} \frac{2C_F}{Q^2} \delta^+(M_L^2) \frac{\delta(\omega - \omega')}{\omega\omega'} \frac{f(\epsilon)}{e^{-\epsilon\gamma_E} \Gamma(1 - \epsilon)} \omega \left(\frac{M_R^2 \omega}{Q\mu^2} \right)^{-\epsilon}. \end{aligned} \quad (3.49)$$

In the B-type term (3.47), the divergence of the convolution arises from small momentum fraction. The integrand of the r, r' integrals in the limit of small r reads

$$\begin{aligned} & \frac{\alpha_s}{4\pi} \frac{2C_F}{Q^2} f(\epsilon) \int dl_+ dl_- \delta^+(M_L^2 - Ql_-) \delta(l_+) \delta(l_-) \\ & \times \frac{\delta(r - r')}{rr'} \frac{1}{\Gamma(1 - \epsilon)} r \left(\frac{(M_R^2 - Ql_+) r}{\mu^2 e^{\gamma_E}} \right)^{-\epsilon} \\ & = \frac{\alpha_s}{4\pi} \frac{2C_F}{Q^2} \delta^+(M_L^2) \frac{\delta(r - r')}{rr'} \frac{f(\epsilon)}{\Gamma(1 - \epsilon)} r \left(\frac{M_R^2 r}{\mu^2 e^{\gamma_E}} \right)^{-\epsilon}, \end{aligned} \quad (3.50)$$

which is identical to the previous expression provided we identify $r = \omega/Q$, $r' = \omega'/Q$. A similar agreement holds for the identical soft anti-quark contribution to the A-type term and the $r \rightarrow 1$ limit of the B-type term (3.47). From the heuristic discussion of section 2 it is evident that this agreement is not a coincidence, but holds to all orders in the expansion in α_s .

4 Endpoint factorization

Eqs. (3.24), (3.44) provide factorized expressions for the two-hemisphere mass distribution in the two-jet limit in the gluon-thrust region from which the NLP logarithms can be computed to any logarithmic accuracy order by order in α_s by evaluating the convolutions of the d -dimensional hard, (anti-)collinear and soft function. The limit $\epsilon \rightarrow 0$ must be taken at the end, because the convolutions in the A-type term are divergent when ω and ω' both tend to infinity. In the B-type term this happens when r and r' both approach 0 or 1.

This form is not quite sufficient to sum the logarithms to all orders in α_s . To apply the standard SCET renormalization-group method to the hard, (anti-)collinear and soft factors, one must renormalize them and take the limit $\epsilon \rightarrow 0$ before the convolution. In this section we employ the coincidence of the integrands in certain asymptotic limits, which should hold on physics grounds and has been demonstrated above at lowest order, to factorize and rearrange the endpoint contributions such that the convolution integrals are finite. Similar methods to derive endpoint factorization at the level of factorization formulas with

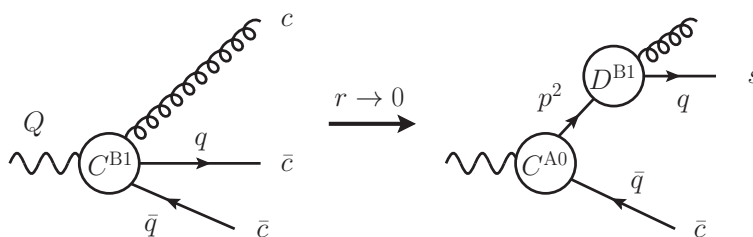


Figure 3. Graphical representation of the factorization (4.1) of the B1 matching coefficient in the soft-quark limit.

functions defined by matrix elements of operators have been derived before only for exclusive B decays to P-wave charmonia [34], which involves SCET and non-relativistic QCD, and Higgs decay to two photons [22], which is a SCET_{II} process. These are amplitude-factorization problems. The present case of gluon thrust is somewhat different as it is a SCET_I problem, and involves inclusive collinear and soft functions defined at cross-section level, similar to [18]. Nevertheless, the main mechanism that achieves endpoint factorization is similar to the above-mentioned cases. Interestingly, it partly involves functions, which are the non-abelian generalization of some that appear in $H \rightarrow \gamma\gamma$.

4.1 Soft-collinear limit of the B1 matching coefficients

An important ingredient in this discussion is the factorization property of the coefficient function of $q\bar{q}g$ SCET B1 operators, when the light-cone momentum fraction carried by the quark or anti-quark becomes small. The endpoint divergence in the B-type contribution originates from the singular behaviour of the C_i^{B1} matching coefficients in this limit, which in turn arises because the intermediate quark or anti-quark goes on-shell, see figure 1.

By its original definition, the matching coefficient is a single-scale, hard function. For $r \rightarrow 0$ (soft quark) and $r \rightarrow 1$ (soft anti-quark), it becomes a two-scale object, which can itself be factorized according to [18]

$$C_1^{\text{B1}}(Q^2, r) = C^{\text{A0}}(Q^2) \times \frac{D^{\text{B1}}(rQ^2)}{r} + \mathcal{O}(r^0), \quad (4.1)$$

where the two scales Q^2 and rQ^2 are now separated into the hard matching coefficient of the leading-power A0 SCET current, and a new coefficient $D^{\text{B1}}(rQ^2)$, which depends only on the endpoint-scale $\sqrt{r}Q$. We recall that $C_1^{\text{B1}}(Q^2, r)$ is regular in the soft anti-quark limit $r \rightarrow 1$. An analogous factorization holds for the second B1 operator in the limit $r \rightarrow 1$:

$$C_2^{\text{B1}}(Q^2, r) = -C^{\text{A0}}(Q^2) \times \frac{D^{\text{B1}}(\bar{r}Q^2)}{\bar{r}} + \mathcal{O}(\bar{r}^0). \quad (4.2)$$

Since the two cases are related by $r \leftrightarrow \bar{r}$ (plus a global minus sign), the following is phrased for the soft-quark limit only. A graphical representation of (4.1) is shown in figure 3.

For $r \rightarrow 0$ the outgoing quark represented by $\bar{\chi}_{\bar{c}}$ field in the second line of (3.7) becomes soft-anticollinear. The soft-collinear coefficient $D^{\text{B1}}(p^2)$, which appears in (4.1), (4.2), can

be defined by matching the time-ordered product [18]

$$\langle g_c^a(p_c) q_{\overline{s\bar{c}}}(p_{\overline{s\bar{c}}}) | \int d^4x T \{ \bar{\chi}_c(0), \mathcal{L}_{\xi q}(x) \} | 0 \rangle = g_s \bar{u}(p_{\overline{s\bar{c}}}) t^a \not{\epsilon}_{c\perp}(p_c) \frac{i n_+ p_c \not{n}_-}{p^2} \frac{\not{n}_-}{2} D^{\text{B1}}(p^2), \quad (4.3)$$

with $p^2 = (p_c + p_{\overline{s\bar{c}}})^2 = rQ^2$ and

$$\mathcal{L}_{\xi q}(x) = \bar{q}_{\overline{s\bar{c}}}(x_-) \mathcal{A}_{c\perp}(x) \chi_c(x) + \text{h.c.} \quad (4.4)$$

the leading soft-quark Lagrangian [26, 27] with \bar{q}_s replaced by $\bar{q}_{\overline{s\bar{c}}}$. This relation becomes evident by comparing the second diagram in figure 2 to the right-hand side in figure 3. From its definition in terms of a time-ordered product it is clear that the matching coefficient $D^{\text{B1}}(p^2)$ is a universal function that will appear in different processes involving soft quark emission.

The leading double-logarithmic resummation of $D^{\text{B1}}(p^2)$ to all orders in α_s has been derived in [18]. It exhibits the all-order $(C_A - C_F)^n$ colour coefficient, which seems to be characteristic for soft quark emission [14, 18, 35]. Interestingly, the same coefficient enters the ggH amplitude with a bottom-quark loop and was recently computed at the two-loop level [36], together with its one-loop evolution kernel, which was obtained from renormalization-group invariance of the full ggH amplitude.

The $D^{\text{B1}}(p^2)$ coefficient as well as its evolution equation can also be obtained from the corresponding B1 operator coefficients and anomalous dimension by taking the limit $r \rightarrow 0$. Since the anti-collinear part of the B1 operator has the same field content as the operator relevant to light-cone distribution amplitudes, the extraction of the anomalous dimension is similar to the derivation of the asymptotic kernel for the QED light-meson light-cone distribution amplitude [37], see also [22]. We refer to appendix A for this derivation, which results in

$$D^{\text{B1}}(p^2) = 1 + \frac{\alpha_s}{4\pi} (C_F - C_A) \left(\frac{2}{\epsilon^2} - 1 - \frac{\pi^2}{6} \right) \left(\frac{\mu^2}{-p^2 - i\epsilon} \right)^\epsilon + \mathcal{O}(\alpha_s^2). \quad (4.5)$$

$$\frac{d}{d \ln \mu} D^{\text{B1}}(p^2) = \int_0^\infty d\hat{p}^2 \gamma_D(\hat{p}^2, p^2) D^{\text{B1}}(\hat{p}^2), \quad (4.6)$$

with

$$\begin{aligned} \gamma_D(\hat{p}^2, p^2) &= \frac{\alpha_s (C_F - C_A)}{\pi} \delta(\hat{p}^2 - p^2) \ln \left(\frac{\mu^2}{-p^2 - i\epsilon} \right) \\ &\quad + \frac{\alpha_s}{\pi} \left(\frac{C_A}{2} - C_F \right) p^2 \left[\frac{\theta(\hat{p}^2 - p^2)}{\hat{p}^2(\hat{p}^2 - p^2)} + \frac{\theta(p^2 - \hat{p}^2)}{p^2(p^2 - \hat{p}^2)} \right]_+, \end{aligned} \quad (4.7)$$

in agreement with [36].

When the gluon field is replaced by a photon, the corresponding abelian version of $D^{\text{B1}}(p^2)$ is identical to the jet function, which appears at LP in the factorization of the radiative semi-leptonic B decay $B \rightarrow \gamma \ell \nu$ [38] and in the NLP endpoint factorization of the photonic Higgs decay $H \rightarrow \gamma \gamma$ amplitude through a bottom-quark loop [22]. In the abelian case, the two-loop evolution has been inferred from renormalization-group consistency of the $B \rightarrow \gamma \ell \nu$ observable [39]. The direct computation of the one-loop evolution kernel of this jet function can be found in [40].

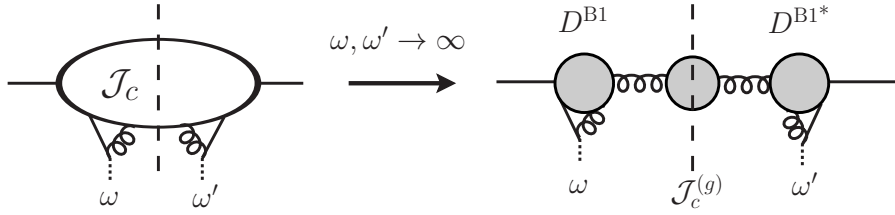


Figure 4. Factorization of the radiative collinear function $\mathcal{J}_c(p^2, \omega, \omega')$, which appears in the A-type term, in the limit $\omega, \omega' \rightarrow \infty$.

4.2 Endpoint factorization consistency conditions

As discussed in section 2 and checked explicitly above at $\mathcal{O}(\alpha_s)$, we expect the integrand of the A- and B-type terms of the factorization formula to have identical asymptotic limits to all orders, which is a prerequisite for endpoint factorization. More precisely, the limit of anti-collinear momentum component $n_- \cdot p_c = rQ, r'Q \rightarrow 0$ in the B-type term, matches the limit $n_- \cdot k = \omega, \omega' \rightarrow \infty$ of the corresponding soft momentum component in the A-type term.¹⁰

We start from the expressions (3.27), (3.45) in Laplace space, in which the integrand of the ω, ω' and r, r' integrals involves no further integrals and the consistency relations are algebraic. The coincidence of asymptotic limits implies that the following must hold:

$$\begin{aligned} & \frac{2C_F}{Q^2} f(\epsilon) C_1^{\text{B1}*}(Q^2, r') C_1^{\text{B1}}(Q^2, r) \tilde{\mathcal{J}}_c^{q\bar{q}(8)}(s_R, r, r') \tilde{\mathcal{J}}_c^{(g)}(s_L) \tilde{\mathcal{S}}^{(g)}(s_R, s_L) \Big|_{r^{(\prime)} = \frac{\omega^{(\prime)}}{Q} \rightarrow 0} \\ &= \frac{2C_F}{Q} f(\epsilon) |C^{\text{A0}}(Q^2)|^2 \tilde{\mathcal{J}}_c^{(\bar{q})}(s_R) \times \left\{ \tilde{\mathcal{J}}_c(s_L, \omega, \omega') \tilde{\mathcal{S}}_{\text{NLP}}(s_R, s_L, \omega, \omega') \right. \\ & \quad \left. + \tilde{\tilde{\mathcal{J}}}_c(s_L, \omega, \omega') \tilde{\tilde{\mathcal{S}}}_{\text{NLP}}(s_R, s_L, \omega, \omega') \right\} \Big|_{\omega, \omega' \rightarrow \infty}. \end{aligned} \quad (4.8)$$

The left-hand side of this equation represents the leading asymptotics of the B-type term (3.45) for $r, r' \rightarrow 0$, already accounting for the fact that this arises only from the square of the amplitude of the first B1 operator, since the coefficient of the second is non-singular as $r \rightarrow 0$. The right-hand side is one half of the total A-type term, which we can identify with the soft quark contribution. An analogous equation with $r, r' \rightarrow \bar{r}, \bar{r}'$ and $C_1^{\text{B1}} \rightarrow C_2^{\text{B1}}$ applies to the limit $r, r' \rightarrow 1$. The right-hand side of (4.8) contains two terms in the curly brackets, which correspond to different colour structure in the jet and soft function, (3.17) and (3.20), respectively. We shall now show that endpoint factorization consistency implies that the hatted term in (4.8) is subleading as $\omega, \omega' \rightarrow \infty$, and can be dropped.

We recall from (3.17) that $\mathcal{J}_c(p^2, \omega, \omega')$ is an inclusive radiative jet function of the non-local, time-ordered product operator defined in (3.16). Graphically, we may represent it by the diagram to the left of the arrow in figure 4, where the dashed external lines to the left

¹⁰There is a similar matching of the limit $(1-r)Q, (1-r')Q \rightarrow 0$ with the soft *anti*-quark contribution to the A-type term. This contribution can be treated as below, after changing variables from $r^{(\prime)} \rightarrow 1 - r^{(\prime)}$.

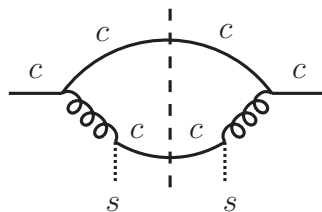


Figure 5. Example of a one-collinear-particle reducible diagram, which does not contribute to the large- $\omega^{(\prime)}$ behaviour of $\mathcal{J}_c(p^2, \omega, \omega')$.

and right of the cut denote the *soft* momentum of the composite field $\mathcal{A}_{\perp c} \chi_c$ in the time-ordered product, which is carried away by the soft quark. We now claim that the leading asymptotic behaviour proportional to $1/(\omega\omega')$ for large ω, ω' requires that the diagram is “one-collinear-particle reducible”, as displayed to the right of the arrow in figure 4. Then colour conservation implies that the collinear line must be a colour-octet, that is a gluon, and hence only the unhatted colour term (3.17), which defines $\mathcal{J}_c(p^2, \omega, \omega')$ contributes to the asymptotic behaviour, as was to be shown.

Suppose the diagram was not one-collinear-particle reducible, such as the one-loop example displayed in figure 5. Endpoint factorization consistency requires that the large ω, ω' must match a corresponding B-type contribution, obtained by making the dashed lines representing external soft quark anti-collinear. This turns internal collinear propagators into hard propagators, and the entire diagram into a contribution to the matching coefficient of a hard operator with external collinear and anti-collinear fields. The key observation is that if the diagram was not one-collinear-particle reducible, the corresponding hard operator would contain more than one external collinear field, in contradiction with the B1 operators available at NLP, which contain only a single collinear gluon field, see (3.7). Consistency therefore requires that the asymptotic behaviour takes the diagrammatic form shown in figure 4. This proves not only that the hatted jet function is irrelevant for endpoint factorization, but further that $\mathcal{J}_c(p^2, \omega, \omega')$ factorizes into the product¹¹

$$(I) \quad \mathcal{J}_c(p^2, \omega, \omega') = \mathcal{J}_c^{(g)}(p^2) \frac{D^{\text{B1}}(\omega Q)}{\omega} \frac{D^{\text{B1}^*}(\omega' Q)}{\omega'} + \mathcal{O}\left(\frac{1}{\omega^{(\prime)}}\right), \quad (4.9)$$

where the function $D^{\text{B1}}(p^2)$ is the same as the one that appears in the factorization of the hard B1 operator coefficient (4.1).

Eq. (4.9) is the first endpoint factorization consistency condition. Inserting the Laplace-transformed version of this relation together with (4.1) for the B1 hard function into (4.8) immediately implies a similar consistency relation for the NLP soft quark function,

$$(II) \quad Q \tilde{\mathcal{J}}_{\tilde{c}}^{(\tilde{q})}(s_R) \tilde{\mathcal{S}}_{\text{NLP}}(s_R, s_L, \omega, \omega') \Big|_{\omega^{(\prime)} \rightarrow \infty} \\ = \tilde{\mathcal{J}}_{\tilde{c}}^{q\tilde{q}^{(8)}}(s_R, r, r') \tilde{\mathcal{S}}^{(g)}(s_R, s_L) \Big|_{r^{(\prime)} = \omega^{(\prime)}/Q \rightarrow 0}. \quad (4.10)$$

¹¹The collinear scale on the left-hand side is $n_+ p^{(\prime)} = Q\omega^{(\prime)}$, but we suppressed the factor of Q in the respective arguments of $\mathcal{J}_c(p^2, \omega, \omega')$.

The same identity holds with $r, r' \rightarrow \bar{r}, \bar{r}'$. Relations (I) and (II) formalize the heuristic picture developed in section 2. For large ω , the soft quark field in S_{NLP} becomes anti-collinear, $\bar{q}_s Y_{n_-} \rightarrow \bar{\chi}_{\bar{c}}$, hence it moves from S_{NLP} to the anti-collinear function $\mathcal{J}_{\bar{c}}^{q\bar{q}(8)}$. Removing $\bar{q}_s Y_{n_-}$ from S_{NLP} leaves the leading-power soft function $S^{(g)}$, while adding it as $\bar{\chi}_{\bar{c}}$ to $\mathcal{J}_{\bar{c}}^{(\bar{q})}$ turns the anti-quark jet function into $\mathcal{J}_{\bar{c}}^{q\bar{q}(8)}$. Overall, this results in $S_{\text{NLP}} \mathcal{J}_{\bar{c}}^{(\bar{q})} \rightarrow S^{(g)} \mathcal{J}_{\bar{c}}^{q\bar{q}(8)}$, which is relation (II). At the same time, the quark fields in the A-type collinear function (3.16) become highly off-shell, which removes them from $\mathcal{J}_c(p^2, \omega, \omega')$, leaving only the collinear gluon, and consequently C^{A0} turns into C^{B1} . Thus, $|C^{\text{A0}}|^2 \mathcal{J}_c \rightarrow |C^{\text{B1}}|^2 \mathcal{J}_c^{(g)}$, which is relation (I).

4.3 Endpoint factorization formula

We are now in the position to derive the endpoint-finite factorization formula. For its concise formulation, we employ the double-bracket notation introduced in [21] to denote the asymptotic behaviours of the various functions. The precise definitions are as follows: in functions of ω, ω' , rescale $\omega \rightarrow \kappa\omega, \omega' \rightarrow \kappa\omega'$ and take $\kappa \rightarrow \infty$. Then

$$\llbracket S_{\text{NLP}}(l_+, l_-, \omega, \omega') \rrbracket \equiv S_{\text{NLP}}(l_+, l_-, \omega, \omega')|_{\mathcal{O}(\kappa^0)}, \quad (4.11)$$

$$\llbracket \mathcal{J}_c(p^2, \omega, \omega') \rrbracket \equiv \mathcal{J}_c(p^2, \omega, \omega')|_{\mathcal{O}(\kappa^{-2})}, \quad (4.12)$$

where $\delta(\omega - \omega')$ counts as κ^{-1} . The right-hand side of the previous equation equals the right-hand side of the consistency relation (I). Similarly, in functions of r, r' , rescale $r \rightarrow r\kappa, r' \rightarrow r'\kappa$ and take $\kappa \rightarrow 0$, or the corresponding rescaling is applied to \bar{r}, \bar{r}' . Which of the two is meant, will be indicated by the subscript 0 or 1 on the double bracket. Then

$$\llbracket C_1^{\text{B1}}(Q^2, r) \rrbracket_0 \equiv C_1^{\text{B1}}(Q^2, r)|_{\mathcal{O}(\kappa^{-1})}, \quad (4.13)$$

$$\llbracket C_2^{\text{B1}}(Q^2, r) \rrbracket_1 \equiv C_2^{\text{B1}}(Q^2, r)|_{\mathcal{O}(\kappa^{-1})}, \quad (4.14)$$

while $\llbracket C_1^{\text{B1}}(Q^2, r) \rrbracket_1 = \llbracket C_2^{\text{B1}}(Q^2, r) \rrbracket_0 = 0$. With this definition the right-hand sides of these equations are given by (4.1) and (4.2), respectively. Finally, we have

$$\llbracket \mathcal{J}_{\bar{c}}^{q\bar{q}(8)}(p^2, r, r') \rrbracket_0 = \llbracket \mathcal{J}_{\bar{c}}^{q\bar{q}(8)}(p^2, r, r') \rrbracket_1 \equiv \mathcal{J}_{\bar{c}}^{q\bar{q}(8)}(p^2, r, r')|_{\mathcal{O}(\kappa^0)} \quad (4.15)$$

due to the symmetry $r^{(l)} \leftrightarrow \bar{r}^{(l)}$. In the d -dimensional expressions there are ϵ -dependent powers of κ , which turn into logarithms in the renormalized functions. Thus ϵ counts as an infinitesimal variable for the purpose of endpoint κ power-counting.

To implement the rearrangement of endpoint-singular terms we start with the scaleless integral

$$\begin{aligned} & \frac{2C_F}{Q} f(\epsilon) |C^{\text{A0}}(Q^2)|^2 \tilde{\mathcal{J}}_{\bar{c}}^{(\bar{q})}(s_R) \tilde{\mathcal{J}}_c^{(g)}(s_L) \\ & \times \int_0^\infty d\omega d\omega' \frac{D^{\text{B1}}(\omega Q)}{\omega} \frac{D^{\text{B1}*}(\omega' Q)}{\omega'} \llbracket \tilde{S}_{\text{NLP}}(s_R, s_L, \omega, \omega') \rrbracket, \end{aligned} \quad (4.16)$$

which vanishes in d dimensions. We split this integral in two terms $I_{1,2}$, which can be done in two ways, illustrated in figure 6: (1) ω and ω' smaller than an endpoint factorization

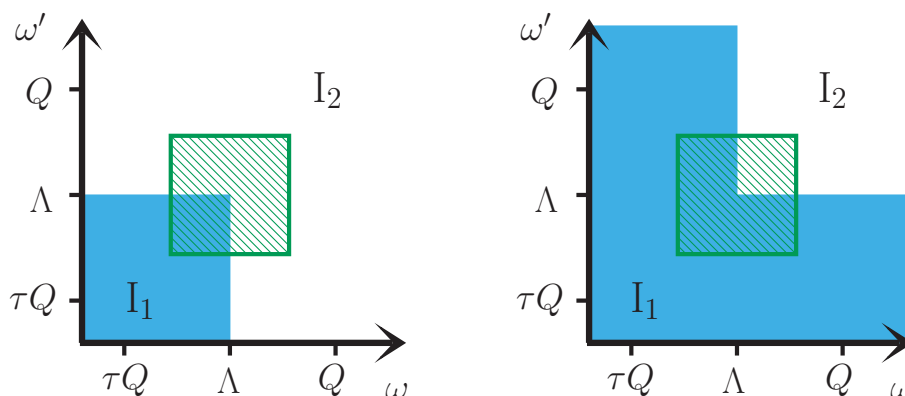


Figure 6. Version (1) [left] and (2) [right] of the split of (4.16) into $I_1 + I_2$ according to the correspondingly indicated regions in the $\omega - \omega'$ plane as described in the text below (4.16). In the overlap region in green the asymptotic behaviour of the A- and B-type term must agree.

parameter Λ (integral I_1), and the complement region I_2 . (2) ω or ω' smaller Λ and the complement region. Since the mixed regions where one variable is larger and the other smaller than Λ are not endpoint-singular, both ways could be employed for the following considerations, although the expressions take a different form. We will use the second version. In this case the complement region is $\omega, \omega' > \Lambda$ and the double-bracket asymptotic behaviour can be used for functions of ω, ω' in the A-type term.¹² In both versions $I_1 + I_2 = 0$. The endpoint rearrangement now consists of subtracting I_1 from the B-type term and I_2 from the A-type term. The subtracted expressions are now separately endpoint-finite, but depend on Λ . However, as long as no approximations are made, the Λ dependence cancels exactly between the two terms.

We begin with the A-type contribution (3.27), which accounts for soft-quark emission, to the factorization theorem and subtract from it the complement region I_2 , $\omega, \omega' > \Lambda$, of the integral (4.16), resulting in

$$\begin{aligned}
 \frac{1}{\sigma_0} \frac{d\tilde{\sigma}}{ds_R ds_L} \Big|_{\text{A-type}} &= \frac{2C_F}{Q} f(\epsilon) |C^{A0}(Q^2)|^2 \tilde{\mathcal{J}}_c^{(\bar{q})}(s_R) \int_0^\infty d\omega d\omega' \\
 &\times \left\{ \tilde{\mathcal{J}}_c(s_L, \omega, \omega') \tilde{\mathcal{S}}_{\text{NLP}}(s_R, s_L, \omega, \omega') \right. \\
 &\quad - \theta(\omega - \Lambda) \theta(\omega' - \Lambda) \tilde{\mathcal{J}}_c^{(g)}(s_L) \frac{D^{\text{B1}}(\omega Q)}{\omega} \frac{D^{\text{B1}^*}(\omega' Q)}{\omega'} \left[\tilde{\mathcal{S}}_{\text{NLP}}(s_R, s_L, \omega, \omega') \right] \\
 &\quad \left. + \tilde{\mathcal{J}}_c(s_L, \omega, \omega') \tilde{\mathcal{S}}_{\text{NLP}}(s_R, s_L, \omega, \omega') \right\}. \tag{4.17}
 \end{aligned}$$

For $\omega, \omega' \rightarrow \infty$, we use the endpoint factorization condition (I) from (4.9) to rewrite the jet function in the first term of the integrand. In this limit it is also justified to replace the soft function by its asymptotic form (4.11). Thus the first and second term in the integrand

¹²While in version (1), it could be used for functions of r, r' in the B-type term with identification $r^{(\prime)} = \omega^{(\prime)}/Q$. The resulting expressions for this version are provided in appendix B.

cancel. The third term is subleading in this limit, and the convolution integrals over ω and ω' are now endpoint-finite, as the logarithmically divergent part of the integrand in the large ω and ω' region has been removed. To make this explicit, we use (4.9) in (4.17), and obtain

$$\begin{aligned} \frac{1}{\sigma_0} \frac{\widetilde{d\sigma}}{ds_R ds_L} \Big|_{\text{A-type}} &= \frac{2C_F}{Q} f(\epsilon) |C^{A0}(Q^2)|^2 \widetilde{\mathcal{J}}_c^{(\bar{q})}(s_R) \int_0^\infty d\omega d\omega' \\ &\times \left\{ \widetilde{\mathcal{J}}_c(s_L, \omega, \omega') \widetilde{S}_{\text{NLP}}(s_R, s_L, \omega, \omega') \right. \\ &\quad - \theta(\omega - \Lambda)\theta(\omega' - \Lambda) \llbracket \widetilde{\mathcal{J}}_c(s_L, \omega, \omega') \rrbracket \llbracket \widetilde{S}_{\text{NLP}}(s_R, s_L, \omega, \omega') \rrbracket \\ &\quad \left. + \widetilde{\mathcal{J}}_c(s_L, \omega, \omega') \widetilde{S}_{\text{NLP}}(s_R, s_L, \omega, \omega') \right\}. \end{aligned} \quad (4.18)$$

If we further choose $\Lambda \gg 1/s_R, 1/s_L$, we may simplify the previous equation to

$$\begin{aligned} \frac{1}{\sigma_0} \frac{\widetilde{d\sigma}}{ds_R ds_L} \Big|_{\text{A-type}} &= \frac{2C_F}{Q} f(\epsilon) |C^{A0}(Q^2)|^2 \widetilde{\mathcal{J}}_c^{(\bar{q})}(s_R) \int_0^\infty d\omega d\omega' \\ &\times \left\{ \left[1 - \theta(\omega - \Lambda)\theta(\omega' - \Lambda) \right] \widetilde{\mathcal{J}}_c(s_L, \omega, \omega') \widetilde{S}_{\text{NLP}}(s_R, s_L, \omega, \omega') \right. \\ &\quad \left. + \widetilde{\mathcal{J}}_c(s_L, \omega, \omega') \widetilde{S}_{\text{NLP}}(s_R, s_L, \omega, \omega') \right\} \\ &= \frac{2C_F}{Q} f(\epsilon) |C^{A0}(Q^2)|^2 \widetilde{\mathcal{J}}_c^{(\bar{q})}(s_R) \int d\omega d\omega' \left[1 - \theta(\omega - \Lambda)\theta(\omega' - \Lambda) \right] \\ &\times \left\{ \widetilde{\mathcal{J}}_c(s_L, \omega, \omega') \widetilde{S}_{\text{NLP}}(s_R, s_L, \omega, \omega') + \widetilde{\mathcal{J}}_c(s_L, \omega, \omega') \widetilde{S}_{\text{NLP}}(s_R, s_L, \omega, \omega') \right\}, \end{aligned} \quad (4.19)$$

where the equality signs hold up to corrections of $\mathcal{O}(1/(s_L\Lambda), 1/(s_R\Lambda))$. It is then understood that in evaluating (4.19), terms suppressed by powers of Λ are dropped. This is simply (3.27) with integration region $\omega, \omega' > \Lambda$ removed, see figure 6.

The remaining part I_1 of the integral (4.16) can now be combined with $i = i' = 1$ part of the B-type term (3.45). Similarly, we proceed for the A-type soft-antiquark contribution and the $i = i' = 2$ part of the B-type term after using the symmetry under the exchange $r \leftrightarrow \bar{r}$. The term $i \neq i'$ is endpoint-finite so it remains unaffected.

Beginning with the $i = i' = 1$ term, we have

$$\begin{aligned} \frac{1}{\sigma_0} \frac{\widetilde{d\sigma}}{ds_R ds_L} \Big|_{\substack{\text{B-type} \\ i=i'=1}} &= \frac{2C_F}{Q^2} f(\epsilon) \left[\widetilde{\mathcal{J}}_c^{(g)}(s_L) \widetilde{S}^{(g)}(s_R, s_L) \right. \\ &\quad \times \int_0^1 dr dr' C_1^{\text{B1}*}(Q^2, r') C_1^{\text{B1}}(Q^2, r) \widetilde{\mathcal{J}}_c^{q\bar{q}(8)}(s_R, r, r') \\ &\quad - Q |C^{A0}(Q^2)|^2 \widetilde{\mathcal{J}}_c^{(\bar{q})}(s_R) \widetilde{\mathcal{J}}_c^{(g)}(s_L) \int_0^\infty d\omega d\omega' \left[1 - \theta(\omega - \Lambda)\theta(\omega' - \Lambda) \right] \\ &\quad \left. \times \frac{D^{\text{B1}}(\omega Q)}{\omega} \frac{D^{\text{B1}*}(\omega' Q)}{\omega'} \llbracket \widetilde{S}_{\text{NLP}}(s_R, s_L, \omega, \omega') \rrbracket \right]. \end{aligned} \quad (4.20)$$

We substitute $\omega = rQ$ and $\omega' = r'Q$ in the subtraction term, and employ (4.1) to express the D^{B1} functions in terms of the asymptotic limits of the B1 matching coefficients. Next,

we make use of the endpoint factorization condition (II) to express the asymptotic soft-quark function in terms of the B-type jet function $\tilde{\mathcal{J}}_c^{q\bar{q}(8)}(s_R, r, r')$ in the asymptotic limit to obtain

$$\begin{aligned} \frac{1}{\sigma_0} \frac{\tilde{d}\sigma}{ds_R ds_L} \Big|_{\substack{\text{B-type} \\ i=i'=1}} &= \frac{2C_F}{Q^2} f(\epsilon) \tilde{\mathcal{J}}_c^{(g)}(s_L) \tilde{S}^{(g)}(s_R, s_L) \int_0^\infty dr dr' \\ &\times \left[\theta(1-r)\theta(1-r') C_1^{\text{B1}*}(Q^2, r') C_1^{\text{B1}}(Q^2, r) \tilde{\mathcal{J}}_c^{q\bar{q}(8)}(s_R, r, r') \right. \\ &\quad - [1 - \theta(r - \Lambda/Q)\theta(r' - \Lambda/Q)] \\ &\quad \left. \times \llbracket C_1^{\text{B1}*}(Q^2, r') \rrbracket_0 \llbracket C_1^{\text{B1}}(Q^2, r) \rrbracket_0 \llbracket \tilde{\mathcal{J}}_c^{q\bar{q}(8)}(s_R, r, r') \rrbracket_0 \right], \quad (4.21) \end{aligned}$$

where now the integrals over r, r' are evaluated from 0 to ∞ . The convolution integrals are now convergent, but they must be evaluated after the integrands are combined. Provided $\Lambda \ll Q$, this expression can be simplified to

$$\begin{aligned} \frac{1}{\sigma_0} \frac{\tilde{d}\sigma}{ds_R ds_L} \Big|_{\substack{\text{B-type} \\ i=i'=1}} &= \frac{2C_F}{Q^2} f(\epsilon) \tilde{\mathcal{J}}_c^{(g)}(s_L) \tilde{S}^{(g)}(s_R, s_L) \\ &\times \left\{ \int_0^1 dr dr' [1 - \theta(\Lambda/Q - r)\theta(\Lambda/Q - r')] C_1^{\text{B1}*}(Q^2, r') C_1^{\text{B1}}(Q^2, r) \tilde{\mathcal{J}}_c^{q\bar{q}(8)}(s_R, r, r') \right. \\ &\quad - \int_0^\infty dr dr' [\theta(r - \Lambda/Q)\theta(\Lambda/Q - r') + \theta(\Lambda/Q - r)\theta(r' - \Lambda/Q)] \\ &\quad \left. \times \llbracket C_1^{\text{B1}*}(Q^2, r') \rrbracket_0 \llbracket C_1^{\text{B1}}(Q^2, r) \rrbracket_0 \llbracket \tilde{\mathcal{J}}_c^{q\bar{q}(8)}(s_R, r, r') \rrbracket_0 \right\}, \quad (4.22) \end{aligned}$$

up to corrections of $\mathcal{O}(\Lambda/Q)$. The first integral in the curly brackets is simply (3.45) with integration region $r, r' < \Lambda/Q$ removed, see figure 6, which is endpoint-finite. The second integral is a finite left-over from the subtraction term.

For completeness, we provide the term $i = i' = 2$. In the bare factorization formula (3.45) we change integration variables to \bar{r}, \bar{r}' to map the singular point $r = r' = 1$ to $\bar{r} = \bar{r}' = 0$. The subtraction term is then obtained after mapping $\omega = \bar{r}Q$ and $\omega' = \bar{r}'Q$ and following the same steps as before we find

$$\begin{aligned} \frac{1}{\sigma_0} \frac{\tilde{d}\sigma}{ds_R ds_L} \Big|_{\substack{\text{B-type} \\ i=i'=2}} &= \frac{2C_F}{Q^2} f(\epsilon) \tilde{\mathcal{J}}_c^{(g)}(s_L) \tilde{S}^{(g)}(s_R, s_L) \int_0^\infty d\bar{r} d\bar{r}' \\ &\times \left[\theta(1-\bar{r})\theta(1-\bar{r}') C_2^{\text{B1}*}(Q^2, r') C_2^{\text{B1}}(Q^2, r) \tilde{\mathcal{J}}_c^{q\bar{q}(8)}(s_R, r, r') \right. \\ &\quad - [1 - \theta(\bar{r} - \Lambda/Q)\theta(\bar{r}' - \Lambda/Q)] \\ &\quad \left. \times \llbracket C_2^{\text{B1}*}(Q^2, r') \rrbracket_1 \llbracket C_2^{\text{B1}}(Q^2, r) \rrbracket_1 \llbracket \tilde{\mathcal{J}}_c^{q\bar{q}(8)}(s_R, r, r') \rrbracket_1 \right], \quad (4.23) \end{aligned}$$

which coincides with (4.21) up to the expected substitutions. Similar simplifications hold when $\Lambda \ll Q$ is assumed. The total endpoint-subtracted B-type is the sum of (4.21), (4.23) and the mixed term $i \neq i'$ in (4.1).

By construction, the dependence on Λ cancels in the sum of the A- and B-type contributions. In appendix B we provide the corresponding version of the endpoint-rearranged factorization formulas, when (4.16) is split according to the first version mentioned below this equation, that is, for ω and ω' smaller than Λ .

5 Renormalization-group equations

In this section we collect the renormalization-group functions, which are known for some of the hard, soft and (anti-) collinear functions of the two terms in the factorization formula, and infer the others from renormalization-group consistency, namely the condition that the renormalized *integrand*s of the A- and B-type term must be separately independent of the scale μ . The endpoint-factorization conditions then provide further relations between the anomalous dimensions in the respective large- ω and small- r limits. We then obtain the solutions to leading-logarithmic (LL) accuracy, which includes running-coupling effects.

5.1 RGEs for the A-type functions

In the A-type term, the hard function and the anti-collinear function are LP objects. Their evolution is therefore well-known. The evolution of the two NLP objects, the collinear function and the soft function, is currently unknown. We cannot reconstruct both RGEs from just consistency arguments since we are missing two anomalous dimensions.

Instead, we will use the endpoint factorization condition (I) from (4.9) to derive the evolution of the collinear function $\mathcal{J}_c(p^2, \omega, \omega')$ for large ω, ω' from the known RGEs for the LP gluon jet function and the D^{B1} coefficient. Through consistency, we can then derive the asymptotic evolution of the soft function. This allows us to resum the A-type functions in the endpoint region, which is sufficient for LL accuracy.

Hard function. The evolution of the LP hard matching coefficient C^{A0} is well known [41]. It obeys the RGE

$$\frac{d}{d \ln \mu} C^{A0}(Q^2, \mu^2) = \left[C_F \gamma_{\text{cusp}}(\alpha_s) \ln \frac{-Q^2}{\mu^2} + \gamma_{A0}(\alpha_s) \right] C^{A0}(Q^2, \mu^2), \quad (5.1)$$

where $-Q^2$ in the logarithm should be read as $-Q^2 - i\varepsilon$. The cusp anomalous dimension γ_{cusp} and the hard non-cusp anomalous dimension γ_{A0} are given by

$$\gamma_{\text{cusp}}(\alpha_s) = 4 \frac{\alpha_s}{4\pi} + \mathcal{O}(\alpha_s^2), \quad (5.2)$$

$$\gamma_{A0}(\alpha_s) = -6C_F \frac{\alpha_s}{4\pi} + \mathcal{O}(\alpha_s^2). \quad (5.3)$$

The one-loop cusp anomalous dimension sums the leading logarithms. Non-cusp terms become relevant only at NLL accuracy.¹³ Dropping them, we obtain the LL solution

$$C_{\text{LL}}^{A0}(Q^2, \mu^2) = \exp[2C_F S(\mu_h, \mu)] \left(\frac{-Q^2}{\mu_h^2} \right)^{-C_F A \gamma_{\text{cusp}}(\mu_h, \mu)} C^{A0}(Q^2, \mu_h^2), \quad (5.4)$$

¹³We make an exception for the non-cusp terms proportional to β_0 , for example in (5.12) below, which determine the scale of the coupling that appears in the tree-level $\mathcal{O}(\alpha_s)$ term. See section 6 for further discussion.

where $\mu_h \sim Q$ denotes the hard initial scale, such that $C^{A0}(Q^2, \mu_h^2)$ free from large logarithms. The functions $S(\nu, \mu)$ and $A_{\gamma_i}(\nu, \mu)$ are defined as [42]

$$S(\nu, \mu) = - \int_{\alpha_s(\nu)}^{\alpha_s(\mu)} d\alpha \frac{\gamma_{\text{cusp}}(\alpha)}{\beta(\alpha)} \int_{\alpha_s(\nu)}^{\alpha} d\alpha' \frac{1}{\beta(\alpha')}, \quad (5.5)$$

$$A_{\gamma_i}(\nu, \mu) = - \int_{\alpha_s(\nu)}^{\alpha_s(\mu)} d\alpha \frac{\gamma_i(\alpha)}{\beta(\alpha)}. \quad (5.6)$$

The QCD beta-function is

$$\beta(\alpha_s) = \frac{d\alpha_s}{d \ln \mu} = -2\beta_0 \frac{\alpha_s^2}{4\pi} + \mathcal{O}(\alpha_s^3), \quad \beta_0 = 11 - \frac{2n_l}{3}. \quad (5.7)$$

Anti-collinear function. The anti-collinear function appears already at LP. In Laplace space, it obeys the local RGE [41]

$$\frac{d}{d \ln \mu} \tilde{\mathcal{J}}_{\bar{c}}^{(\bar{q})}(s, Q^2, \mu^2) = - \left[2C_F \gamma_{\text{cusp}}(\alpha_s) \ln \frac{Q}{s e^{\gamma_E} \mu^2} + \gamma_{\mathcal{J}(\bar{q})}(\alpha_s) \right] \tilde{\mathcal{J}}_{\bar{c}}^{(\bar{q})}(s, Q^2, \mu^2), \quad (5.8)$$

where the non-cusp term is given by

$$\gamma_{\mathcal{J}(\bar{q})}(\alpha_s) = -6C_F \frac{\alpha_s}{4\pi} + \mathcal{O}(\alpha_s^2). \quad (5.9)$$

At LL accuracy, the RGE is solved by

$$\tilde{\mathcal{J}}_{\bar{c}, \text{LL}}^{(\bar{q})}(s, Q^2, \mu^2) = \exp[-4C_F S(\mu_{\bar{c}}, \mu)] \left(\frac{Q}{s e^{\gamma_E} \mu_{\bar{c}}^2} \right)^{2C_F A_{\gamma_{\text{cusp}}}(\mu_{\bar{c}}, \mu)} \tilde{\mathcal{J}}_{\bar{c}}^{(\bar{q})}(s, Q^2, \mu_{\bar{c}}^2), \quad (5.10)$$

where $\mu_{\bar{c}}$ denotes the anti-collinear initial scale.

Collinear function. The collinear function $\mathcal{J}_c(p^2, \omega, \omega')$ is a new NLP object and its anomalous dimension is currently unknown. In the asymptotic region of large ω, ω' , it factorizes into the LP gluon jet function and two D^{B1} matching coefficients as shown in (4.9). We therefore derive its asymptotic evolution from the LP gluon jet function, which renormalizes in Laplace space as [43]

$$\frac{d}{d \ln \mu} \tilde{\mathcal{J}}_c^{(g)}(s, Q^2, \mu^2) = - \left[2C_A \gamma_{\text{cusp}}(\alpha_s) \ln \frac{Q}{s e^{\gamma_E} \mu^2} + \gamma_{\mathcal{J}(g)}(\alpha_s) \right] \tilde{\mathcal{J}}_c^{(g)}(s, Q^2, \mu^2), \quad (5.11)$$

with the gluon non-cusp term given by

$$\gamma_{\mathcal{J}(g)}(\alpha_s) = -2\beta_0 \frac{\alpha_s}{4\pi} + \mathcal{O}(\alpha_s^2), \quad (5.12)$$

and the evolution of the D^{B1} coefficient. Making the cusp term explicit, (4.6), (4.7) or (A.29), (A.30) imply the non-local RGE

$$\begin{aligned} \frac{d}{d \ln \mu} D^{B1}(\omega, \mu^2) &= - (C_F - C_A) \gamma_{\text{cusp}}(\alpha_s) \ln \frac{-\omega Q - i\varepsilon}{\mu^2} D^{B1}(\omega, \mu^2) \\ &\quad + \int_0^\infty d\hat{\omega} \hat{\gamma}_D(\hat{\omega}, \omega) D^{B1}(\hat{\omega}, \mu^2), \end{aligned} \quad (5.13)$$

where the non-cusp anomalous dimension $\hat{\gamma}_D(\hat{\omega}, \omega)$ is given by the second line of (A.30). The first endpoint factorization consistency condition (4.9) now implies the following asymptotic RGE for the collinear function \mathcal{J}_c ,

$$\begin{aligned}
 \frac{d}{d \ln \mu} \left[\tilde{\mathcal{J}}_c(s, \omega, \omega', Q^2, \mu^2) \right] &= - \left[2C_A \gamma_{\text{cusp}}(\alpha_s) \ln \frac{Q}{s e^{\gamma_E} \mu^2} \right. \\
 &\quad \left. + (C_F - C_A) \gamma_{\text{cusp}}(\alpha_s) \left(\ln \frac{\omega Q}{\mu^2} + \ln \frac{\omega' Q}{\mu^2} \right) \right] \left[\tilde{\mathcal{J}}_c(s, \omega, \omega', Q^2, \mu^2) \right] \\
 &\quad - \gamma_{\mathcal{J}(g)}(\alpha_s) \left[\tilde{\mathcal{J}}_c(s, \omega, \omega', Q^2, \mu^2) \right] + \int_0^\infty d\hat{\omega} \frac{\hat{\omega}}{\omega} \hat{\gamma}_D(\hat{\omega}, \omega) \left[\tilde{\mathcal{J}}_c(s, \hat{\omega}, \omega', Q^2, \mu^2) \right] \\
 &\quad + \int_0^\infty d\hat{\omega}' \frac{\hat{\omega}'}{\omega'} \hat{\gamma}_D^*(\hat{\omega}', \omega') \left[\tilde{\mathcal{J}}_c(s, \omega, \hat{\omega}', Q^2, \mu^2) \right]. \tag{5.14}
 \end{aligned}$$

There is no mixing of the unhatted collinear function into the hatted collinear function, which is irrelevant asymptotically. At LL accuracy, we drop the non-cusp terms (except for those proportional to β_0) and obtain the solution

$$\begin{aligned}
 \left[\tilde{\mathcal{J}}_{c, \text{LL}}(s, \omega, \omega', Q^2, \mu^2) \right] &= \frac{\alpha_s(\mu_c)}{\alpha_s(\mu)} \exp[-4C_A S(\mu_c, \mu) - 4(C_F - C_A) S(\mu_{c\Lambda}, \mu)] \\
 &\quad \times \left(\frac{Q}{s e^{\gamma_E} \mu_c^2} \right)^{2C_A A_{\gamma_{\text{cusp}}}(\mu_c, \mu)} \left(\frac{\omega Q}{\mu_{c\Lambda}^2} \right)^{(C_F - C_A) A_{\gamma_{\text{cusp}}}(\mu_{c\Lambda}, \mu)} \\
 &\quad \times \left(\frac{\omega' Q}{\mu_{c\Lambda}^2} \right)^{(C_F - C_A) A_{\gamma_{\text{cusp}}}(\mu_{c\Lambda}, \mu)} \left[\tilde{\mathcal{J}}_c(s, \omega, \omega', Q^2, \mu_c^2, \mu_{c\Lambda}^2) \right]. \tag{5.15}
 \end{aligned}$$

We introduce two initial scales, μ_c and $\mu_{c\Lambda}$, connected to the two different cusp logarithms in (5.14), allowing for the possibility to choose different initial scales for the gluon jet function and D^{B1} coefficient, which will be used in section 6.1.

Soft function. The soft quark function $S_{\text{NLP}}(l_+, l_-, \omega, \omega')$ appears first at NLP and its complete RGE is currently unknown even at lowest order. We can obtain its asymptotic evolution for large ω, ω' from RGE consistency. For fixed values of ω, ω' and r, r' , respectively, the integrands of the A- and B-type terms must be individually RGE-invariant. Imposing this requirement on the A-type term, we obtain the asymptotic RGE for the soft function,

$$\begin{aligned}
 \frac{d}{d \ln \mu} \left[\tilde{S}_{\text{NLP}}(s_R, s_L, \omega, \omega', \mu^2) \right] &= \left[2C_A \gamma_{\text{cusp}}(\alpha_s) \ln \frac{1}{s_L e^{\gamma_E} s_R e^{\gamma_E} \mu^2} \right. \\
 &\quad \left. + (C_F - C_A) \gamma_{\text{cusp}}(\alpha_s) \left(\ln \frac{\omega}{s_R e^{\gamma_E} \mu^2} + \ln \frac{\omega'}{s_R e^{\gamma_E} \mu^2} \right) \right] \left[\tilde{S}_{\text{NLP}}(s_R, s_L, \omega, \omega', \mu^2) \right] \\
 &\quad + \left[\gamma_{\mathcal{J}(\bar{q})}(\alpha_s) + \gamma_{\mathcal{J}(g)}(\alpha_s) - 2\gamma_{A0}(\alpha_s) \right] \left[\tilde{S}_{\text{NLP}}(s_R, s_L, \omega, \omega', \mu^2) \right] \\
 &\quad - \int_0^\infty d\hat{\omega} \frac{\hat{\omega}}{\omega} \hat{\gamma}_D(\hat{\omega}, \omega) \left[\tilde{S}_{\text{NLP}}(s_R, s_L, \hat{\omega}, \omega', \mu^2) \right] \\
 &\quad - \int_0^\infty d\hat{\omega}' \frac{\hat{\omega}'}{\omega'} \hat{\gamma}_D^*(\hat{\omega}', \omega') \left[\tilde{S}_{\text{NLP}}(s_R, s_L, \omega, \hat{\omega}', \mu^2) \right]. \tag{5.16}
 \end{aligned}$$

Consistency requires that there is no mixing of the unhatted soft function into the hatted soft function. At LL accuracy, the asymptotic RGE is solved by

$$\begin{aligned}
 \left[\tilde{S}_{\text{NLP,LL}}(s_R, s_L, \omega, \omega', \mu^2) \right] &= \frac{\alpha_s(\mu)}{\alpha_s(\mu_s)} \exp [4C_A S(\mu_s, \mu) + 4(C_F - C_A) S(\mu_{s\Lambda}, \mu)] \\
 &\times \left(\frac{1}{s_L e^{\gamma_E} s_R e^{\gamma_E} \mu_s^2} \right)^{-2C_A A_{\gamma_{\text{cusp}}}(\mu_s, \mu)} \left(\frac{\omega}{s_R e^{\gamma_E} \mu_{s\Lambda}^2} \right)^{-(C_F - C_A) A_{\gamma_{\text{cusp}}}(\mu_{s\Lambda}, \mu)} \\
 &\times \left(\frac{\omega'}{s_R e^{\gamma_E} \mu_{s\Lambda}^2} \right)^{-(C_F - C_A) A_{\gamma_{\text{cusp}}}(\mu_{s\Lambda}, \mu)} \left[\tilde{S}_{\text{NLP}}(s_R, s_L, \omega, \omega', \mu_s^2, \mu_{s\Lambda}^2) \right], \quad (5.17)
 \end{aligned}$$

where again we allow for two separate initial soft scales, μ_s and $\mu_{s\Lambda}$. The lowest-order initial condition is proportional to α_s , which we choose to evaluate at μ_s . Together with the prefactor $\alpha_s(\mu)/\alpha_s(\mu_s)$, which arises from the β_0 -term in $\gamma_{\mathcal{J}(g)}$, this results in an overall factor of $\alpha_s(\mu)$. The point of keeping the non-cusp β_0 -term in $\gamma_{\mathcal{J}(g)}$ is that it renders the result independent of the initial scale — choosing to evaluate α_s at $\mu_{s\Lambda}$ instead, we would obtain the same resummed soft function.

5.2 RGEs for the B-type functions

In the B-type contribution, the collinear function and the soft function are known LP objects while the hard functions C_i^{B1} and the anti-collinear function $\mathcal{J}_{\bar{c}}^{q\bar{q}(8)}(p^2, r, r')$ are NLP objects. The evolution equation of the hard matching coefficients is of the form discussed in [44, 45] for B1 SCET operators, hence we can derive the anomalous dimensions for the new anti-collinear function from consistency, i.e. the scale-independence of the entire B-type term for given r, r' . However, the leading logarithms to gluon thrust arise only from the endpoint region $r, r' \rightarrow 0, 1$, and therefore we will only need the equations for the asymptotic hard and anti-collinear functions.

Collinear function. The anomalous dimension of the collinear function is well-known since it appears in LP factorization theorems. The RGE and anomalous dimension have already been given in (5.11) and (5.12), respectively. The LL solution to the RGE reads

$$\tilde{\mathcal{J}}_{c,\text{LL}}^{(g)}(s, \mu^2) = \frac{\alpha_s(\mu_c)}{\alpha_s(\mu)} \exp[-4C_A S(\mu_c, \mu)] \left(\frac{Q}{s e^{\gamma_E} \mu_c^2} \right)^{2C_A A_{\gamma_{\text{cusp}}}(\mu_c, \mu)} \tilde{\mathcal{J}}_c^{(g)}(s, \mu_c^2), \quad (5.18)$$

where μ_c denotes the collinear initial scale.

Soft function. The LP two-hemisphere soft function for gluons, which is defined with adjoint Wilson lines, obeys the evolution equation

$$\frac{d}{d \ln \mu} \tilde{S}^{(g)}(s_R, s_L, \mu^2) = \left[2C_A \gamma_{\text{cusp}}(\alpha_s) \ln \frac{1}{s_L s_R e^{2\gamma_E} \mu^2} + \gamma_{S^{(g)}}(\alpha_s) \right] \tilde{S}^{(g)}(s_R, s_L, \mu^2) \quad (5.19)$$

in Laplace space. The non-cusp part of the anomalous dimension is given by [46]

$$\gamma_{S^{(g)}}(\alpha_s) = 0 + \mathcal{O}(\alpha_s^2). \quad (5.20)$$

At LL accuracy, the solution to the RGE reads

$$\begin{aligned} \tilde{S}_{\text{LL}}^{(g)}(s_R, s_L, \mu^2) &= \exp[4C_A S(\mu_s, \mu)] \left(\frac{1}{s_L s_R e^{2\gamma_E} \mu_s^2} \right)^{-2C_A A_{\gamma_{\text{cusp}}}(\mu_s, \mu)} \\ &\times \tilde{S}^{(g)}(s_R, s_L, \mu_s^2), \end{aligned} \quad (5.21)$$

where μ_s denotes the soft initial scale.

Hard function. Following the calculations of [44, 45], the specific anomalous dimension matrix for the two coefficients C_i^{B1} , $i = 1, 2$ needed here can be inferred from appendix A.2. For the flavour non-singlet case, which is assumed here, Δ_F can be set to zero there, and the two coefficients evolve independently,

$$\frac{d}{d \ln \mu} C_i^{\text{B1}}(Q^2, r) = \int_0^1 d\hat{r} \gamma_{\text{B1}}(\hat{r}, r) C_i^{\text{B1}}(Q^2, \hat{r}), \quad (5.22)$$

with the same anomalous dimension (see (A.14))

$$\gamma_{\text{B1}}(r, s) = -\frac{\alpha_s}{\pi} \delta(r-s) \left[C_A \ln \left(\frac{\mu^2}{-Q^2} \right) - \frac{C_A}{2} \ln(r\bar{r}) + \frac{3C_F}{2} \right] + 2\gamma(r, s), \quad (5.23)$$

where

$$\begin{aligned} \gamma(r, s) &= \frac{\alpha_s}{2\pi} \left(\frac{C_A}{2} - C_F \right) \left[\frac{\bar{r}}{\bar{s}} \left(\left(\frac{\theta(r-s)}{r-s} \right)_+ + \theta(r-s) \right) \right. \\ &\quad \left. + \frac{r}{s} \left(\left(\frac{\theta(s-r)}{s-r} \right)_+ + \theta(s-r) \right) \right]. \end{aligned} \quad (5.24)$$

The non-cusp part of this RGE contains a hidden large logarithm of r (\bar{r}), which must be extracted and combined with the cusp part when one wants to sum the hard function for small r or \bar{r} , see appendix A.2. This results in the evolution equation (4.6) for the D^{B1} coefficient. The evolution equation for the asymptotic C_i^{B1} coefficients then follows from (4.1), (4.2). Since the leading logarithms to gluon thrust arise only from these asymptotic regions, we provide the RGEs for the asymptotic coefficients in the following.

The asymptotic B1 coefficients factorize into a product of A0 coefficient and the D^{B1} coefficient. Combining (5.1) and (5.13), we find

$$\begin{aligned} \frac{d}{d \ln \mu} \left[C_1^{\text{B1}}(Q^2, r, \mu^2) \right]_0 &= \left[C_F \gamma_{\text{cusp}}(\alpha_s) \ln \frac{-Q^2}{\mu^2} \right. \\ &\quad \left. - (C_F - C_A) \gamma_{\text{cusp}}(\alpha_s) \ln \frac{-rQ^2}{\mu^2} + \gamma_{\text{A0}}(\alpha_s) \right] \left[C_1^{\text{B1}}(Q^2, r, \mu^2) \right]_0 \\ &\quad + Q \int_0^\infty d\hat{r} \frac{\hat{r}}{r} \hat{\gamma}_D(\hat{r}Q, rQ) \left[C_1^{\text{B1}}(Q^2, \hat{r}, \mu^2) \right]_0. \end{aligned} \quad (5.25)$$

The LL solution reads

$$\begin{aligned} \left[C_1^{\text{B1}}(Q^2, r, \mu^2) \right]_0 &= \exp[2C_F S(\mu_h, \mu) - 2(C_F - C_A) S(\mu_{h\Lambda}, \mu)] \\ &\times \left(\frac{-Q^2}{\mu_h^2} \right)^{-C_F A_{\gamma_{\text{cusp}}}(\mu_h, \mu)} \left(\frac{-rQ^2}{\mu_{h\Lambda}^2} \right)^{(C_F - C_A) A_{\gamma_{\text{cusp}}}(\mu_h, \mu)} \\ &\times \left[C_1^{\text{B1}}(Q^2, r, \mu_h^2, \mu_{h\Lambda}^2) \right]_0, \end{aligned} \quad (5.26)$$

where as in the case of similar A-type RGE solutions, we allowed for two different initial scales, μ_h and $\mu_{h\Lambda}$, connected with the different cusp logarithms.

For each of the two endpoint limits $r \rightarrow 0, 1$, we only need one of the two B1 coefficients since the other one is regular. The RGE equation and solution for $C_2^{\text{B1}}(Q^2, r, \mu^2)$ is obtained from the above by replacing $r \rightarrow \bar{r}$, and similarly for \hat{r} including the integration measure $d\hat{r}$.

Anti-collinear function. The evolution of the hard, collinear, and soft functions is known, hence we can derive the evolution of the anti-collinear function through consistency. We demand that the B-type contribution before integration over r, r' is RGE-invariant on its own, which allows us to derive the RGE and anomalous dimension of the anti-collinear function in the form

$$\begin{aligned} \frac{d}{d\ln\mu} \tilde{\mathcal{J}}_{\bar{c}}^{q\bar{q}(8)}(s_R, r, r') &= \left[-2C_A \gamma_{\text{cusp}}(\alpha_s) \ln \frac{Q}{s_R e^{\gamma_E} \mu^2} \right. \\ &\quad \left. + \gamma_{\mathcal{J}(g)}(\alpha_s) - \gamma_{S(g)}(\alpha_s) \right] \tilde{\mathcal{J}}_{\bar{c}}^{q\bar{q}(8)}(s_R, r, r') \\ &\quad - \int_0^1 d\hat{r} \hat{\gamma}_{\text{B1}}(r, \hat{r}) \tilde{\mathcal{J}}_{\bar{c}}^{q\bar{q}(8)}(s_R, \hat{r}, r') - \int_0^1 d\hat{r}' \hat{\gamma}_{\text{B1}}^*(r', \hat{r}') \tilde{\mathcal{J}}_{\bar{c}}^{q\bar{q}(8)}(s_R, r, \hat{r}'), \end{aligned} \quad (5.27)$$

where the non-cusp part of the B1 anomalous dimension $\hat{\gamma}_{\text{B1}}$ is given by

$$\hat{\gamma}_{\text{B1}}(r, s) = \frac{\alpha_s}{\pi} \delta(r - s) \left[\frac{C_A}{2} \ln(r\bar{r}) - \frac{3C_F}{2} \right] + 2\gamma(r, s). \quad (5.28)$$

As for the hard function, the non-cusp part of the full anomalous dimension contains hidden leading logarithms coming from the endpoint region. We therefore use asymptotic anomalous dimensions for the LL resummation. RGE-consistency yields in the two endpoint regions

$$\begin{aligned} \frac{d}{d\ln\mu} \left[\tilde{\mathcal{J}}_{\bar{c}}^{q\bar{q}(8)}(s, r, r', \mu^2) \right]_0 &= - \left[2C_F \gamma_{\text{cusp}}(\alpha_s) \ln \frac{Q}{s e^{\gamma_E} \mu^2} \right. \\ &\quad \left. - (C_F - C_A) \gamma_{\text{cusp}}(\alpha_s) \left(\ln \frac{rQ}{s e^{\gamma_E} \mu^2} + \ln \frac{r'Q}{s e^{\gamma_E} \mu^2} \right) \right. \\ &\quad \left. + [2\gamma_{A0}(\alpha_s) + \gamma_{S(g)}(\alpha_s) - \gamma_{\mathcal{J}(g)}(\alpha_s)] \right] \left[\tilde{\mathcal{J}}_{\bar{c}}^{q\bar{q}(8)}(s, r, r', \mu^2) \right]_0 \\ &\quad - Q \int_0^\infty d\hat{r} \frac{r}{\hat{r}} \hat{\gamma}_D(rQ, \hat{r}Q) \left[\tilde{\mathcal{J}}_{\bar{c}}^{q\bar{q}(8)}(s, \hat{r}, r', \mu^2) \right]_0 \\ &\quad - Q \int_0^\infty d\hat{r}' \frac{r'}{\hat{r}'} \hat{\gamma}_D^*(r'Q, \hat{r}'Q) \left[\tilde{\mathcal{J}}_{\bar{c}}^{q\bar{q}(8)}(s, r, \hat{r}', \mu^2) \right]_0. \end{aligned} \quad (5.29)$$

At LL accuracy, the asymptotic RGE is solved by

$$\begin{aligned} \left[\tilde{\mathcal{J}}_{\bar{c}, \text{LL}}^{q\bar{q}(8)}(s, r, r', \mu^2) \right]_0 &= \frac{\alpha_s(\mu)}{\alpha_s(\mu_{\bar{c}})} \exp[-4C_F S(\mu_{\bar{c}}, \mu) + 4(C_F - C_A) S(\mu_{\bar{c}\Lambda}, \mu)] \\ &\quad \times \left(\frac{Q}{s e^{\gamma_E} \mu_{\bar{c}}^2} \right)^{2C_F A \gamma_{\text{cusp}}(\mu_{\bar{c}}, \mu)} \left(\frac{rQ}{s e^{\gamma_E} \mu_{\bar{c}\Lambda}^2} \right)^{-(C_F - C_A) A \gamma_{\text{cusp}}(\mu_{\bar{c}\Lambda}, \mu)} \\ &\quad \times \left(\frac{r'Q}{s e^{\gamma_E} \mu_{\bar{c}\Lambda}^2} \right)^{-(C_F - C_A) A \gamma_{\text{cusp}}(\mu_{\bar{c}\Lambda}, \mu)} \left[\tilde{\mathcal{J}}_{\bar{c}}^{q\bar{q}(8)}(s, r, r', \mu_{\bar{c}}^2, \mu_{\bar{c}\Lambda}^2) \right]_0, \end{aligned} \quad (5.30)$$

where $\mu_{\bar{c}}$ and $\mu_{\bar{c}\Lambda}$ denote the anti-collinear initial scales. As for the A-type soft function, we may evaluate the factor of α_s in the fixed-order initial condition either at $\mu_{\bar{c}}$ or $\mu_{\bar{c}\Lambda}$, and $\mu_{\bar{c}}$ has been chosen above. This choice does not affect the overall resummed anti-collinear function since the ratio of couplings in front always guarantees a global factor of $\alpha_s(\mu)$. Once again the RGE and solution for the anti-collinear function for $r \rightarrow 1$, $[\tilde{\mathcal{J}}_{\bar{c},\text{LL}}^{q\bar{q}(8)}(s, r, r', \mu^2)]_1$, are obtained from the above by replacing $r \rightarrow \bar{r}$, and similarly for \hat{r} including the integration measure $d\hat{r}$ as well as for the corresponding primed quantities.

6 Resummation

With the individual functions resummed to LL accuracy, we proceed to the resummation of the leading logarithms of gluon thrust at NLP. All functions are renormalized, so from now on we set $d = 4$.

We begin by rearranging the endpoint-subtracted expressions (4.18) and (4.21) for the A- and B-type term, respectively. In (4.18), we rewrite

$$\begin{aligned} & \tilde{\mathcal{J}}_c(s_L, \omega, \omega') \tilde{S}_{\text{NLP}}(s_R, s_L, \omega, \omega') \\ &= \tilde{\mathcal{J}}_c(s_L, \omega, \omega') \tilde{S}_{\text{NLP}}(s_R, s_L, \omega, \omega') - \sigma(\omega, \omega') \left[\tilde{\mathcal{J}}_c(s_L, \omega, \omega') \right] \left[\tilde{S}_{\text{NLP}}(s_R, s_L, \omega, \omega') \right] \\ & \quad + \sigma(\omega, \omega') \left[\tilde{\mathcal{J}}_c(s_L, \omega, \omega') \right] \left[\tilde{S}_{\text{NLP}}(s_R, s_L, \omega, \omega') \right], \end{aligned} \quad (6.1)$$

where $\sigma(\omega, \omega')$ is an auxiliary function, which equals unity whenever $\omega^{(\prime)} s_R, \omega^{(\prime)} s_L \gg 1$ and which goes to zero for $\omega^{(\prime)} \rightarrow 0$. We find

$$\begin{aligned} & \frac{1}{\sigma_0} \frac{d\tilde{\sigma}}{ds_R ds_L} |_{\text{A-type}} = \frac{2C_F}{Q} |C^{\text{A0}}(Q^2)|^2 \tilde{\mathcal{J}}_{\bar{c}}^{(\bar{q})}(s_R) \int_0^\infty d\omega d\omega' \\ & \quad \times \left\{ [\sigma(\omega, \omega') - \theta(\omega - \Lambda)\theta(\omega' - \Lambda)] \left[\tilde{\mathcal{J}}_c(s_L, \omega, \omega') \right] \left[\tilde{S}_{\text{NLP}}(s_R, s_L, \omega, \omega') \right] \right. \\ & \quad + \left[\tilde{\mathcal{J}}_c(s_L, \omega, \omega') \tilde{S}_{\text{NLP}}(s_R, s_L, \omega, \omega') - \sigma(\omega, \omega') \left[\tilde{\mathcal{J}}_c(s_L, \omega, \omega') \right] \left[\tilde{S}_{\text{NLP}}(s_R, s_L, \omega, \omega') \right] \right] \\ & \quad \left. + \tilde{\mathcal{J}}_c(s_L, \omega, \omega') \tilde{S}_{\text{NLP}}(s_R, s_L, \omega, \omega') \right\}. \end{aligned} \quad (6.2)$$

In this expression, the first line in curly brackets is the subtraction term, which contains the endpoint divergence, if $\Lambda \rightarrow \infty$, and therefore results in a logarithmically enhanced contribution from the ω, ω' convolution. The next term in square brackets resembles a “plus-distribution” type term — this combination has no support for large ω, ω' and does not produce an extra logarithm. Finally, the last term in curly brackets involving the hatted soft function is regular by itself and does not require subtraction. After this rewriting, only the first line in curly brackets needs to be kept at LL accuracy. The introduction of the auxiliary function σ is necessary to eliminate a spurious singularity for small ω, ω' , which arises if one wants to integrate the subtraction and plus-distribution-like term separately, and which cancels between the two.

Similarly, we write (4.21) in the form

$$\begin{aligned}
 \frac{1}{\sigma_0} \frac{d\tilde{\sigma}}{ds_R ds_L} \Big|_{\substack{\text{B-type} \\ i=i'=1}} &= \frac{2C_F}{Q^2} \tilde{J}_c^{(g)}(s_L) \tilde{S}^{(g)}(s_R, s_L) \\
 &\times \left\{ \int_0^\infty dr dr' \left[\theta(1-r)\theta(1-r') - 1 + \theta\left(r - \frac{\Lambda}{Q}\right)\theta\left(r' - \frac{\Lambda}{Q}\right) \right] \right. \\
 &\quad \times \left[C_1^{\text{B1}*}(Q^2, r') \right]_0 \left[C_1^{\text{B1}}(Q^2, r) \right]_0 \left[\tilde{\mathcal{J}}_{\bar{c}}^{q\bar{q}(8)}(s_R, r, r') \right]_0 \\
 &\quad + \int_0^1 dr dr' \left[C_1^{\text{B1}*}(Q^2, r') C_1^{\text{B1}}(Q^2, r) \tilde{\mathcal{J}}_{\bar{c}}^{q\bar{q}(8)}(s_R, r, r') \right. \\
 &\quad \left. \left. - \left[C_1^{\text{B1}*}(Q^2, r') \right]_0 \left[C_1^{\text{B1}}(Q^2, r) \right]_0 \left[\tilde{\mathcal{J}}_{\bar{c}}^{q\bar{q}(8)}(s_R, r, r') \right]_0 \right] \right\}. \quad (6.3)
 \end{aligned}$$

The first integral in curly brackets represents the subtraction term, which contributes to the leading logarithms and cancels the Λ -dependence of the corresponding A-type term. The second integral with support in $[0, 1]$ is of the plus-distribution type and can be safely integrated to $r, r' = 0$. This term can be dropped at LL accuracy. An auxiliary function is not required for the B-type term.

We remind the reader that there is an identical soft anti-quark A-type term and the $i = i' = 2$ term, which is identical to the $i = i' = 1$ term due to the symmetry in $r^{(l)} \leftrightarrow \bar{r}^{(l)}$. The $i \neq i'$ interference terms can be dropped at this point for LL accuracy.

The previous two equations are general and provide a suitable starting point for the resummation of NLP logarithms beyond the leading ones. Since some of the non-asymptotic anomalous dimensions in the plus-distribution-like terms are not yet available, the following focuses on the leading logarithms, including a new set of next-to-leading logarithms associated with the running coupling in the leading terms.

6.1 Counting of logarithms and proper choice of scales

Standard Sudakov exponentiation puts an observable into the form

$$I \sim F(\alpha_s) \exp(\ln \tau g_0(\lambda) + g_1(\lambda) + \alpha_s g_2(\lambda) + \dots), \quad (6.4)$$

where $\lambda = \alpha_s \ln \tau$ counts as $\mathcal{O}(1)$, while $\tau \ll 1$. The function g_0 is needed to sum the leading logarithms, g_1 is NLL etc. F collects the initial condition and has an expansion without large logs. The $\mathcal{O}(\alpha_s)$ correction to the leading approximation of F is already a next-to-next-to-leading logarithmic (NNLL) effect. The large-logarithm counting primarily refers to the *exponent*.

The *integrands* of (6.2), (6.3) are of this form when the solutions to the RGEs from section 5 are used. However, one now has to take integrals of the form

$$\int_{\tau Q}^{\Lambda} \frac{d\omega}{\omega} I(\omega), \quad \int_{\Lambda/Q}^1 \frac{dr}{r} I(r), \quad (6.5)$$

and the assumption underlying standard Sudakov resummation that $\omega = \mathcal{O}(\tau)$ and $r = \mathcal{O}(1)$ is not justified, since either $\Lambda \gg \tau Q$ or $\Lambda \ll Q$, or both. The fact that the integrals are

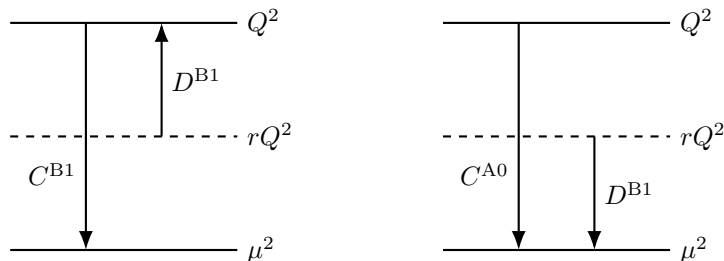


Figure 7. Graphical illustration of the resummation of the initial condition of the B1 operator for $r \ll 1$ (left) and the LL-accurate approximate procedure employed here.

logarithmic for large ω and small r implies two modifications of the standard resummation scheme.

First, the logarithmic integrals combine to an extra logarithm promoting their log-counting by one order. Thus, inserting the LL-resummed RGE functions in the subtraction terms in (6.2), (6.3) will result in leading logarithms for the observables. On the other hand, inserting them into the plus-distribution type terms will result only in next-to-leading logarithms, since these terms are not sensitive to the large ω and small r region by construction and therefore lack one power of logarithm. This counting extends to higher logarithmic order in an obvious manner and justifies the previous assertion that to LL accuracy, it suffices to focus on the subtraction terms in (6.2), (6.3).

Second, the fact that $\omega = \mathcal{O}(\tau)$ and $r = \mathcal{O}(1)$ cannot be assumed can be seen as the need for resumming the initial condition of the RGE evolution. Consider for example the hard function $C_1^{B1}(Q^2, r, \mu^2)$. Standard RGE summation implies that in the initial condition, one chooses the scale $\mu_h \sim Q$, at which there are no large logarithms and evolves to $\mu \ll Q$. However, the initial condition for $\mu_h \sim Q$ may still contain an infinite series of $\ln r$ terms. While these normally count as $\mathcal{O}(1)$, they lead to a breakdown of the perturbative expansion in integrals such as (6.5), which receive contributions from $r \ll 1$. These logarithms are summed by evolving with asymptotic evolution kernel for the D^{B1} coefficient from $\mu^2 \sim rQ^2$ to μ_h^2 . At LL accuracy, combining this evolution with the standard evolution from μ_h to μ , amounts to the expression (5.26) with split initial scales — $\mu_h \sim Q$ in C^{A0} , and the running scale $\mu_{h\Lambda}^2 \sim rQ^2$ for the part that arises from the D^{B1} coefficient, whose natural scale is rQ^2 . The procedure is illustrated in figure 7. A similar reasoning applies to the choice of initial conditions for the anti-collinear function $\tilde{\mathcal{J}}_c^{q\bar{q}(8)}(s_R, r, r')$ and the functions $\tilde{\mathcal{J}}_c(s_L, \omega, \omega', Q^2, \mu^2)$, $\tilde{\mathcal{S}}_{\text{NLP}}(s_R, s_L, \omega, \omega', \mu^2)$, which appear in the A-type term. Hence, we choose the initial scales in the hard, soft and (anti-) collinear functions to be of the order of

$$\begin{aligned}
 \mu_h^2 &\sim Q^2, & \mu_c^2 &\sim \frac{Q}{s_L}, & \mu_{\bar{c}}^2 &\sim \frac{Q}{s_R}, & \mu_s^2 &\sim \frac{1}{s_L s_R}, \\
 \mu_{h\Lambda}^2 &\sim rQ^2, & \mu_{c\Lambda}^2 &\sim \omega Q, & \mu_{\bar{c}\Lambda}^2 &\sim \frac{rQ}{s_R}, & \mu_{s\Lambda}^2 &\sim \frac{\omega}{s_R}.
 \end{aligned}
 \tag{6.6}$$

To ensure the cancellation of the rearrangement scale Λ between the A- and B-type terms,

the integrands of the subtractions terms must match, which requires

$$\mu_{s\Lambda} \sim \mu_{\bar{c}\Lambda} \quad \text{and} \quad \mu_{h\Lambda} \sim \mu_{c\Lambda}, \quad (6.7)$$

which is satisfied by (6.6) with the identification $rQ \leftrightarrow \omega$.

We now insert the resummed functions from section 5, evolved from their respective initial scales to a common scale μ , into the *integrands* of (6.2), (6.3), and simplify the expressions employing the identities

$$A_{\gamma_i}(\mu_1, \mu_2) + A_{\gamma_i}(\mu_2, \mu_3) = A_{\gamma_i}(\mu_1, \mu_3), \quad (6.8)$$

$$S(\mu_1, \mu_2) + S(\mu_2, \mu_3) = S(\mu_1, \mu_3) + \ln \frac{\mu_1}{\mu_2} A_{\gamma_{\text{cusp}}}(\mu_2, \mu_3), \quad (6.9)$$

and the special case $\mu_3 = \mu_1$. We also abbreviate $A \equiv A_{\gamma_{\text{cusp}}}$. We find

$$\begin{aligned} & \left| C^{A0}(Q^2) \right|^2 \tilde{\mathcal{J}}_{\bar{c}}^{(\bar{q})}(s_R, Q^2) \left[\tilde{\mathcal{J}}_{\bar{c}}(s_L, \omega, \omega') \right] \left[\tilde{S}_{\text{NLP}}(s_R, s_L, \omega, \omega') \right] \\ &= \exp [4C_F S(\mu_h, \mu_{\bar{c}}) + 4C_A S(\mu_s, \mu_c) + 4(C_F - C_A) S(\mu_{s\Lambda}, \mu_{c\Lambda})] \\ & \times \left(\frac{Q^2}{\mu_h^2} \right)^{-2C_F A(\mu_h, \mu_{\bar{c}})} \left(\frac{1}{s_L s_R e^{2\gamma_E} \mu_s^2} \right)^{-2C_A A(\mu_s, \mu_c)} \left(\frac{\omega}{s_R e^{\gamma_E} \mu_{s\Lambda}^2} \right)^{-2(C_F - C_A) A(\mu_{s\Lambda}, \mu_{c\Lambda})} \\ & \times (s_R e^{\gamma_E} Q)^{2C_F A(\mu_{c\Lambda}, \mu_{\bar{c}}) + 2C_A A(\mu_c, \mu_{c\Lambda})} \left[\frac{\alpha_s(\mu_c)}{4\pi} \delta(\omega - \omega') \frac{1}{\omega s_R} \right] \end{aligned} \quad (6.10)$$

for the A-type integrand, and for the B-type, we find

$$\begin{aligned} & \left[C_1^{\text{B1}}(Q^2, r) \right]_0 \left[C_1^{\text{B1*}}(Q^2, r') \right]_0 \tilde{\mathcal{J}}_{\bar{c}}^{(g)}(s_L) \left[\tilde{\mathcal{J}}_{\bar{c}}^{q\bar{q}(8)}(s_R, r, r') \right]_0 \tilde{S}^{(g)}(s_R, s_L) \\ &= \exp [4C_F S(\mu_h, \mu_{\bar{c}}) + 4C_A S(\mu_s, \mu_c) + 4(C_F - C_A) S(\mu_{\bar{c}\Lambda}, \mu_{h\Lambda})] \\ & \times \left(\frac{Q^2}{\mu_h^2} \right)^{-2C_F A(\mu_h, \mu_{\bar{c}})} \left(\frac{1}{s_L s_R e^{2\gamma_E} \mu_s^2} \right)^{-2C_A A(\mu_s, \mu_c)} \left(\frac{rQ}{s_R e^{\gamma_E} \mu_{\bar{c}\Lambda}^2} \right)^{-2(C_F - C_A) A(\mu_{\bar{c}\Lambda}, \mu_{h\Lambda})} \\ & \times (s_R e^{\gamma_E} Q)^{2C_F A(\mu_{h\Lambda}, \mu_{\bar{c}}) + 2C_A A(\mu_c, \mu_{h\Lambda})} \left[\frac{\alpha_s(\mu_c)}{4\pi} \delta(r - r') \frac{Q}{r s_R} \right]. \end{aligned} \quad (6.11)$$

As it should be with all functions evaluated consistently to LL accuracy the above expressions are manifestly independent of the arbitrary renormalization scale μ . Note that if we had not included the terms proportional to β_0 in the non-cusp parts of the anomalous dimensions, the only change would be that the overall prefactor of α_s in the square bracket in (6.10) would be evaluated at scale μ_s (or $\mu_{s\Lambda}$) instead of μ_c . Similarly, in (6.11) the prefactor would be evaluated at $\mu_{\bar{c}}$ (or $\mu_{\bar{c}\Lambda}$) instead of μ_c . The scale at which the prefactor is evaluated formally contributes at the same order in the logarithmic counting as the LL terms in the argument of the exponential factors, when including the running coupling. Therefore, it is necessary to take into account the terms proportional to β_0 in the non-cusp parts of the anomalous dimensions to obtain a consistent LL result. In addition, we note that this also ensures that the final result is insensitive to a possible redefinition $\tilde{\mathcal{J}}_{\bar{c}}^{q\bar{q}(8)} \rightarrow \tilde{\mathcal{J}}_{\bar{c}}^{q\bar{q}(8)}/\alpha_s$ and $C_1^{\text{B1}} \rightarrow C_1^{\text{B1}} \times \sqrt{\alpha_s}$, that corresponds to a reshuffling of the overall factor of α_s from the anti-collinear to the hard function, and similar ambiguities in the definitions of the functions in the A-type term.

We note the similarity between the two expressions. In fact, enforcing the relations (6.7), both expressions are exactly equal up to an overall factor of Q with the identification $\omega^{(i)} = r^{(i)}Q$. We thus sum the subtraction terms from (6.2), (6.3), and change variables from r to ω/Q in the B-type contribution (6.3). We also choose the auxiliary function to be of the form $\sigma(\omega, \omega) = \theta(\omega - \sigma)$, where σ is of order $1/s_R$, or $1/s_L$. The two integrals to be added then combine as

$$\int_0^\infty \frac{d\omega}{\omega} [\theta(\omega - \sigma) - \theta(\omega - \Lambda)] + \int_{\Lambda/Q}^1 \frac{dr}{r} = \int_\sigma^Q \frac{d\omega}{\omega}, \quad (6.12)$$

and we obtain

$$\begin{aligned} \frac{1}{\sigma_0} \frac{\widetilde{d\sigma}}{ds_R ds_L} \Big|_{\text{LL}} &= 2 \cdot \frac{2C_F}{Qs_R} \frac{\alpha_s(\mu_c)}{4\pi} \exp[4C_F S(\mu_h, \mu_{\bar{c}}) + 4C_A S(\mu_s, \mu_c)] \\ &\times \left(\frac{Q^2}{\mu_h^2}\right)^{-2C_F A(\mu_h, \mu_{\bar{c}})} \left(\frac{1}{s_L s_R e^{2\gamma_E} \mu_s^2}\right)^{-2C_A A(\mu_s, \mu_c)} \\ &\times \int_\sigma^Q \frac{d\omega}{\omega} \exp[4(C_F - C_A) S(\mu_{s\Lambda}, \mu_{h\Lambda})] \left(\frac{\omega}{s_R e^{\gamma_E} \mu_{s\Lambda}^2}\right)^{-2(C_F - C_A) A(\mu_{s\Lambda}, \mu_{h\Lambda})} \\ &\times (s_R e^{\gamma_E} Q)^{2C_F A(\mu_{h\Lambda}, \mu_{\bar{c}}) + 2C_A A(\mu_c, \mu_{h\Lambda})}, \end{aligned} \quad (6.13)$$

where $\mu_{h\Lambda}^2 \sim \omega Q$ and $\mu_{s\Lambda}^2 \sim \omega/s_R$ according to (6.6). We also added an overall factor of 2 to account for the identical soft anti-quark and $i = i' = 2$ contribution. This is our main result for the LL resummed two-hemisphere invariant mass distribution in the NLP gluon thrust region. The Laplace-space gluon thrust distribution itself is obtained as

$$\frac{1}{\sigma_0} \frac{\widetilde{d\sigma}}{ds} = \frac{1}{\sigma_0} \frac{\widetilde{d\sigma}}{ds_R ds_L} \Big|_{s_R = s_L = s}, \quad (6.14)$$

which follows from (3.4) and the definition of the Laplace transformation.

6.2 Double-logarithmic limit

The double-logarithmic limit corresponds to evaluating the renormalization group functions at leading order in an expansion in α_s :

$$A(\nu, \mu) = -\frac{\alpha_s}{2\pi} \ln \frac{\mu^2}{\nu^2}, \quad (6.15)$$

$$S(\nu, \mu) = -\frac{\alpha_s}{8\pi} \ln^2 \frac{\mu^2}{\nu^2}. \quad (6.16)$$

Setting scales as prescribed by (6.6), the LL result (6.13) simplifies to

$$\begin{aligned} \frac{1}{\sigma_0} \frac{\widetilde{d\sigma}}{ds_R ds_L} &= \frac{\alpha_s C_F}{\pi} \frac{1}{Qs_R} e^{-\frac{\alpha_s C_A}{\pi} \ln(s_L e^{\gamma_E} Q) \ln(s_R e^{\gamma_E} Q)} \int_\sigma^Q \frac{d\omega}{\omega} \left(\frac{\omega}{Q}\right)^{\frac{\alpha_s}{\pi} (C_F - C_A) \ln(s_R e^{\gamma_E} Q)} \\ &= \frac{C_F}{C_F - C_A} \frac{1}{Qs_R \ln(s_R e^{\gamma_E} Q)} \exp \left[-\frac{\alpha_s C_A}{\pi} \ln(s_L e^{\gamma_E} Q) \ln(s_R e^{\gamma_E} Q) \right] \\ &\times \left\{ 1 - \left(\frac{\sigma}{Q}\right)^{\frac{\alpha_s}{\pi} (C_F - C_A) \ln(s_R e^{\gamma_E} Q)} \right\}. \end{aligned} \quad (6.17)$$

The scale of α_s remains undetermined in the double-logarithmic approximation.

To obtain the thrust distribution we set $s_R = s_L = s$ and choose $\sigma = 1/(se^{\gamma_E})$. For the inverse Laplace-transformation from s to $\tau = 1 - T$ we use that the Laplace transform of τ^a is $\Gamma(1 + a)/(sQ)^{1+a}$. Taylor-expanding this relation in a gives

$$\frac{1}{sQ} \ln^n \left(\frac{1}{se^{\gamma_E} Q} \right) \rightarrow \ln^n \tau - \frac{\pi^2}{12} n(n-1) \ln^{n-2} \tau + \mathcal{O}(\ln^{n-3} \tau), \quad (6.18)$$

where the arrow denotes inverse Laplace-transformation. At the double-logarithmic level, the inverse Laplace-transformation is therefore simply accomplished by multiplying with sQ and substituting $se^{\gamma_E} \rightarrow 1/(Q\tau)$ resulting in

$$\frac{1}{\sigma_0} \frac{d\sigma}{d\tau} \Big|_{\text{DL}} = \frac{C_F}{C_F - C_A} \frac{1}{\ln(1/\tau)} e^{-\frac{\alpha_s C_A}{\pi} \ln^2 \tau} \left\{ 1 - e^{-\frac{\alpha_s}{\pi} (C_F - C_A) \ln^2 \tau} \right\}. \quad (6.19)$$

This agrees with the previous result [14, 18], which, however, was obtained through d -dimensional factorization and consistency relations.¹⁴

6.3 Leading logarithms and running coupling effects

The present approach based on renormalized functions satisfying standard RGEs allow us to go beyond the double-logarithmic limit. As a first application, we consider the LL approximation, which includes one-loop running-coupling effects. The RGE functions read

$$A(\nu, \mu) = \frac{2}{\beta_0} \ln \frac{\alpha_s(\mu)}{\alpha_s(\nu)}, \quad (6.20)$$

$$S(\nu, \mu) = \frac{4\pi}{\beta_0^2 \alpha_s(\nu)} \left[1 - \frac{\alpha_s(\nu)}{\alpha_s(\mu)} - \ln \frac{\alpha_s(\mu)}{\alpha_s(\nu)} \right],$$

and the strong coupling α_s at a scale ν is given by

$$\alpha_s(\nu) = \frac{\alpha_s(\mu)}{1 + \frac{\beta_0}{2\pi} \alpha_s(\mu) \ln \frac{\nu}{\mu}} \quad (6.21)$$

in terms of the coupling at a reference scale μ . In the following α_s without argument refers to $\alpha_s(\mu)$.

These expressions are now to be used in (6.13), which upon implementing (6.6) (with “ \sim ” replaced by “ $=$ ” and s_i by $s_i e^{\gamma_E}$) reads¹⁵

$$\begin{aligned} \frac{1}{\sigma_0} \frac{d\tilde{\sigma}}{ds_R ds_L} \Big|_{\text{LL}} &= \frac{\alpha_s(Q/(s_L e^{\gamma_E})) C_F}{\pi} \frac{1}{Q s_R} \\ &\times \exp \left[4C_F S \left(Q^2, \frac{Q}{s_R e^{\gamma_E}} \right) + 4C_A S \left(\frac{1}{s_L s_R e^{2\gamma_E}}, \frac{Q}{s_L e^{\gamma_E}} \right) \right] \\ &\times \int_{\sigma}^Q \frac{d\omega}{\omega} \exp \left[-4(C_F - C_A) S \left(\omega Q, \frac{\omega}{s_R e^{\gamma_E}} \right) \right] \\ &\times (s_R e^{\gamma_E} Q)^{2C_F A(\omega/s_R e^{\gamma_E}, Q/s_R e^{\gamma_E}) + 2C_A A(Q/s_L e^{\gamma_E}, \omega/s_R e^{\gamma_E})}. \quad (6.22) \end{aligned}$$

¹⁴The overall sign of (E.13) in [18] is given incorrectly. The signs of all previous equations leading to (E.13) are, however, correct.

¹⁵In an abuse of notation, we here give the scale arguments of α_s , A and S as μ^2 rather than μ .

This is our main result for the resummed two-hemisphere invariant mass distribution in the gluon-thrust region. The integral over ω can be performed only numerically.

An approximate analytic expression can be obtained by expanding the one-loop running coupling to linear order in β_0 in the exponent and prefactor, resulting in

$$\begin{aligned}
 \frac{1}{\sigma_0} \frac{\widetilde{d\sigma}}{ds_R ds_L} \Big|_{\text{LL}} &= \frac{\alpha_s C_F}{\pi} \frac{1}{Q s_R} \left(1 - \frac{\beta_0 \alpha_s}{4\pi} \ln \frac{Q}{s_L e^{\gamma_E} \mu^2} \right) \\
 &\times \exp \left[-\frac{\alpha_s C_A}{\pi} \ln(s_L e^{\gamma_E} Q) \ln(s_R e^{\gamma_E} Q) \left(1 - \frac{\beta_0 \alpha_s}{4\pi} \ln \frac{Q}{\sqrt{s_R s_L} e^{\gamma_E} \mu^2} \right) \right] \\
 &\times \int_{\sigma}^Q \frac{d\omega}{\omega} \left(\frac{\omega}{Q} \right)^{\frac{\alpha_s}{\pi} (C_F - C_A) \ln(s_R e^{\gamma_E} Q) \left(1 - \frac{\beta_0 \alpha_s}{4\pi} \ln \frac{Q \sqrt{\omega}}{\sqrt{s_R} e^{\gamma_E} \mu^2} \right)} \\
 &= \frac{C_F}{Q s_R} \exp \left[-\frac{\alpha_s C_A}{\pi} \ln(s_L e^{\gamma_E} Q) \ln(s_R e^{\gamma_E} Q) \left(1 - \frac{\beta_0 \alpha_s}{4\pi} \ln \frac{Q}{\sqrt{s_L s_R} e^{\gamma_E} \mu^2} \right) \right] \\
 &\times \frac{\sqrt{2\pi} \left(1 - \frac{\beta_0 \alpha_s}{4\pi} \ln \frac{Q}{s_L e^{\gamma_E} \mu^2} \right)}{\sqrt{\beta_0} \sqrt{C_A - C_F} \sqrt{\ln(s_R e^{\gamma_E} Q)}} (s_R e^{\gamma_E} Q)^{\frac{2(C_F - C_A)}{\beta_0} \left(1 - \frac{\beta_0 \alpha_s}{4\pi} \ln \frac{Q^{\frac{3}{2}}}{\sqrt{s_R} e^{\gamma_E} \mu^2} \right)^2} \\
 &\times \left[\operatorname{erfi} \left(\sqrt{2 \frac{C_A - C_F}{\beta_0} \ln(s_R e^{\gamma_E} Q)} \left(1 - \frac{\beta_0 \alpha_s}{4\pi} \ln \frac{\sigma \sqrt{Q}}{\sqrt{s_R} e^{\gamma_E} \mu^2} \right) \right) \right. \\
 &\left. - \operatorname{erfi} \left(\sqrt{2 \frac{C_A - C_F}{\beta_0} \ln(s_R e^{\gamma_E} Q)} \left(1 - \frac{\beta_0 \alpha_s}{4\pi} \ln \frac{Q^{\frac{3}{2}}}{\sqrt{s_R} e^{\gamma_E} \mu^2} \right) \right) \right], \quad (6.23)
 \end{aligned}$$

where

$$\operatorname{erfi}(x) = -\frac{2i}{\sqrt{\pi}} \int_0^{ix} dt e^{-t^2}. \quad (6.24)$$

Once again, the thrust distribution in Laplace-space is obtained by identifying $s_R = s_L \equiv s$, in which case we also choose $\sigma = 1/(s e^{\gamma_E})$.

To display the effect of resummation and of running coupling effects, we show in the upper panel of figure 8 the gluon-thrust distribution $\frac{1}{\sigma_0} \frac{d\sigma}{d\tau}$ in the leading $\mathcal{O}(\alpha_s)$ approximation (blue-dotted line) and in the resummed double-logarithmic approximation (6.19) (light-blue band). We adopt $Q = m_Z = 91.1876$ GeV corresponding to final states from hadronic Z -boson decay, and $\alpha_s(m_Z) = 0.1179$. The coupling is evolved with one-loop accuracy and $n_l = 5$ according to (6.21). In the leading-order approximation we choose α_s at the collinear scale $\sqrt{\tau}Q$. Since the scale of α_s is not fixed in the double-logarithmic approximation, we vary it from the soft scale τQ to the hard scale Q , which produces the shown band and a considerable uncertainty. For comparison, we also show (light-green band) the numerical inverse Laplace transform of the double-logarithmic approximation (6.17) in Laplace space. To this end, we compute

$$\frac{1}{\sigma_0} \frac{d\sigma}{d\tau} = \frac{Q}{2\pi i} \int_{c-i\infty}^{c+i\infty} ds e^{s\tau Q} \frac{1}{\sigma_0} \frac{\widetilde{d\sigma}}{ds_R ds_L} \Big|_{s_R=s_L=s}, \quad (6.25)$$

where $c > 0$ is chosen to enclose the singularities of the Laplace-space distribution, excluding the one from the Landau pole of the running coupling, which corresponds to the

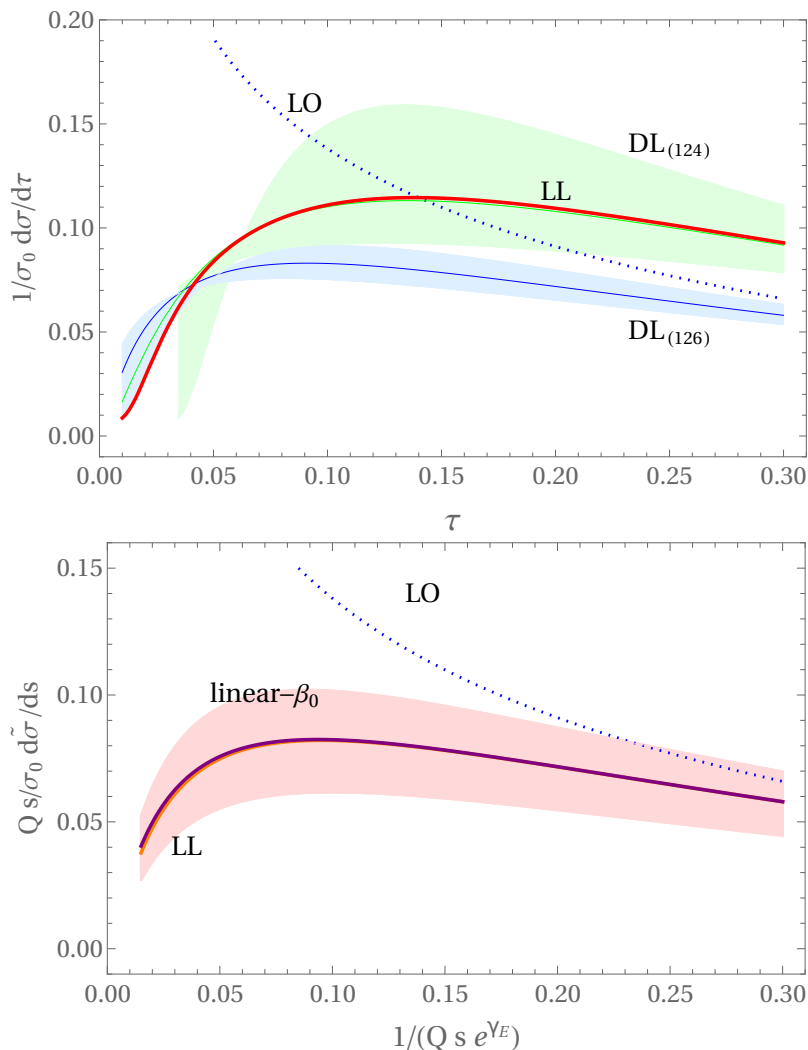


Figure 8. Upper panel: gluon thrust distribution $\frac{1}{\sigma_0} \frac{d\sigma}{d\tau}$ in the double-logarithmic approximation including scale variation (light-blue band from (6.19) and light-green band from the numerical inverse Laplace transform of (6.17)), and the LL approximation (red line). The tree-level result is shown in dotted-blue. Lower panel: Laplace-space gluon thrust distribution (times Q_s), $\frac{Q_s}{\sigma_0} \frac{d\sigma}{ds}$, in the LL approximation (red line), allowing for a variation of the initial scales as described in the text (light-red band). Also shown is the truncation of the LL result to linear order in β_0 from (6.23) (blue), but the difference is hardly visible.

“minimal prescription” of [47]. We also set $\sigma = 1/(se^{\gamma_E})$ in (6.17). We observe a significant difference between the two bands, which must be attributed to formally next-to-leading logarithmic effects in the relation between Laplace and momentum space.

Finally, the upper plot shows (red line) the full leading-logarithmic result (6.22) (with the ω integral evaluated numerically for $\sigma = 1/(se^{\gamma_E})$) after taking the inverse Laplace transformation (6.25) numerically. The LL result turns out to be very close to the DL one when the inverse Laplace transformation is computed in the same way. The green band ends at $\tau \approx 0.03$, since the DL result at the soft scale becomes sensitive to the strong

coupling regime at smaller values τ . We also recall that perturbative resummation requires $Q\tau \gg \Lambda_{\text{QCD}} \approx 0.5 \text{ GeV}$ and $\tau \ll 1$.

We can gain some insight on the importance of intrinsic *next*-to-leading logarithms by varying in the LL result the various matching scales around the values adopted in (6.22). For this purpose, we vary the three pairs of scales $(\mu_h, \mu_{h\Lambda})$, $(\mu_c, \mu_{\bar{c}})$, $(\mu_s, \mu_{s\Lambda})$ by a factor of 1/2 and 2 around their default scales. We then take the minimum and maximum values of the 15 possible combinations of $(1, \frac{1}{2}, \frac{1}{2})$ etc. to compute the scale variation, excluding the cases where different scales are varied in different directions. For simplicity, we show this result for the normalized Laplace-space distribution $\frac{Qs}{\sigma_0} \frac{d\sigma}{ds}$ in the lower panel of figure 8 as the light-red band around the red curve (LL) that represents (6.22). For comparison the tree-level (LO) and linear- β_0 truncation (6.23) of the LL expression are displayed, but the difference between the latter approximation and the full result is hardly visible. The sizeable scale variation seen in the figure emphasizes the need for NLL resummation. The renormalized and endpoint-rearranged factorization formula derived in this work provides the starting point for this systematic improvement. However, the actual implementation requires the calculation of the presently unknown non-cusp parts of the $\mathcal{O}(\alpha_s)$ anomalous dimension of $\mathcal{J}_c(p^2, \omega, \omega')$ and $S_{\text{NLP}}(l_+, l_-, \omega, \omega')$ for general $\omega^{(\prime)}$, which require two-loop calculations beyond the scope of this work, as well as the $\mathcal{O}(\alpha_s^2)$ cusp parts of the anomalous dimensions of the NLP objects.

7 Conclusion

The lack of convergence of the convolution integrals appearing in subleading-power factorization theorems is currently the biggest obstacle to resummation of the power-suppressed large logarithmic corrections in collider physics. This applies in particular to the classic $1 \rightarrow 2$ and $2 \rightarrow 1$ processes, such as event shapes in e^+e^- annihilation, deep-inelastic scattering for $x \rightarrow 1$, and the Drell-Yan threshold.

In earlier work [18] on off-diagonal deep-inelastic scattering for $x \rightarrow 1$, we showed that the hard function of the subleading power B-type operator factorizes in the limit when the collinear momentum fraction carried by one of the quark fields tends to zero. To avoid dealing with the non-perturbative parton distributions, in this work we considered the analogue of the off-diagonal channel for e^+e^- annihilation, “gluon thrust”. Earlier results on the double-logarithmic resummation of this next-to-leading power kinematic configuration employed d -dimensional factorization and consistency relations [14, 18], which do not readily generalize beyond the leading logarithms.

In this paper, we derived a novel endpoint factorization relation for the NLP thrust distribution in the two-jet region for the flavour-nonsinglet off-diagonal contribution, where a gluon-initiated jet recoils against a quark-antiquark pair, which involves subleading-power soft and jet functions defined at the cross-section level. The above-mentioned factorization of the subleading power B-type operator plays again a crucial role for the consistency of the rearrangement that renders the expressions free from endpoint divergences. The framework developed in the present paper allows for the first time to remove systematically endpoint divergences in the convolution integrals of the SCET_I factorization theorems and hence

opens the path to systematic next-to-leading-power resummation for collider observables involving soft quark emission. Employing the subtraction of endpoint divergences with the help of operatorial endpoint factorization conditions, we were able to reshuffle the factorization theorem such that the individual terms are free from endpoint divergences in convolutions and can be expressed in terms of renormalized hard, soft and collinear functions in four dimensions. At this point, standard renormalization-group techniques can be used to obtain the resummed integrands. The basic structure of the rearrangements turns out to be surprisingly similar to the one for Higgs decay through light-quark loops into two photons [21, 22], which however is a SCET_{II} process, where factorization applies to the amplitude. For the $1 \rightarrow 2$ and $2 \rightarrow 1$ processes considered here, there are no rapidity divergences related to momentum modes of the same virtuality, and dimensional regularization suffices to make the convolutions well-defined [10, 15], yet their divergence as $\epsilon \rightarrow 0$ requires rearrangement and refactorization as discussed here.

For the NLP thrust distribution in the power-suppressed two-jet region, where a gluon-initiated jet recoils against a quark-antiquark pair, we derived the necessary anomalous dimension of the NLP jet and soft functions using renormalization-group consistency and endpoint factorization relations. We also explicitly computed the one-loop anomalous dimension for the hard matching coefficients. These ingredients allowed us to perform the first resummation of the endpoint-divergent SCET_I observables at the LL accuracy using exclusively renormalization-group methods. After resummation of the integrands, a judicious choice of initial conditions is necessary for the endpoint-subtraction terms, requiring a scale setting depending on the value of the convolution variable. We verified that our results simplified to double logarithmic accuracy agree with the earlier results [14, 18] and evaluated the numerical impact of the new LL corrections. Our main technical result for gluon thrust is (6.22), which provides a concise expression for the two-hemisphere invariant mass distribution in Laplace space.

The presented method relies on universal properties of the soft and collinear limits and can be applied to other SCET_I problems. An immediate target for the further exploration of NLP resummation is the extension of the present work for gluon thrust and related soft-quark emission processes to NLL accuracy, which requires the computation of renormalization kernels for the NLP soft and jet functions at order $\mathcal{O}(\alpha_s)$, i.e., at the two-loop level (counting phase-space integrals as loops). For the *diagonal* processes, the leading NLP logarithms have been considered for the thrust distribution and the DY threshold in [9, 10, 12, 13], and they turn out to be almost trivial in comparison with the ones for the off-diagonal processes, as there are no endpoint divergences. This is no longer expected beyond the LL accuracy [15]. The present framework supplies a method to address the endpoint divergences that appear in the soft gluon limit at NLP, which is relevant to the diagonal processes.

Acknowledgments

This work has been supported in part by the Excellence Cluster ORIGINS funded by the Deutsche Forschungsgemeinschaft (DFG, German Research Foundation) under Germany's

Excellence Strategy –EXC-2094 –390783311. S.J. is supported by the U.K. Science and Technology Facilities Council (STFC) under grant ST/T001011/1. R.S. is supported by the United States Department of Energy under Grant Contract DE-SC0012704. L.V. is supported by Fellini Fellowship for Innovation at INFN, funded by the European Union’s Horizon 2020 research programme under the Marie Skłodowska-Curie Cofund Action, grant agreement no. 754496. J.W. was supported in part by the National Natural Science Foundation of China (No. 12005117) and the Taishan Scholar Foundation of Shandong province (tsqn201909011). Figures were drawn with Jaxodraw [48].

A C^{B1} and D^{B1}

In this appendix we provide explicit results for the hard matching coefficient $C_i^{\text{B1}}(Q^2, r)$ associated to the SCET operators defined in the second line of (3.7) and (3.10). In momentum space,

$$J_i^{\text{B1}, \mu}(r) = \bar{\chi}_{\bar{c}}(r) \Gamma_i^{\mu\nu} \mathcal{A}_{\nu \perp c} \chi_{\bar{c}}(\bar{r}), \quad i = 1, 2, \quad (\text{A.1})$$

where r and $\bar{r} = 1 - r$ denote the momentum fractions of the anti-collinear quark and anti-quark, respectively, and

$$\Gamma_1^{\mu\nu} = \frac{\not{e}_-}{2} \gamma_{\perp}^{\nu} \gamma_{\perp}^{\mu}, \quad \Gamma_2^{\mu\nu} = \frac{\not{e}_-}{2} \gamma_{\perp}^{\mu} \gamma_{\perp}^{\nu}. \quad (\text{A.2})$$

We then obtain the one-loop correction and one-loop evolution equation of the refactorization coefficient $D^{\text{B1}}(p^2)$ by taking the $r \rightarrow 0$ limit of the corresponding results for $C_1^{\text{B1}}(Q^2, r)$ and (4.1),

$$C_1^{\text{B1}}(Q^2, r) = C^{\text{A0}}(Q^2) \frac{D^{\text{B1}}(rQ^2)}{r} + \text{endpoint-regular}. \quad (\text{A.3})$$

Here endpoint-regular contributions diverge at most logarithmically in the limit $r \rightarrow 0$.

A.1 One-loop results

Allowing for the one-loop correction to (3.30), we write

$$C_1^{\text{B1}}(Q^2, r) = \frac{1}{r} \left(1 + \frac{\alpha_s}{4\pi} \Delta^{\text{B1}}(Q^2, r) + \mathcal{O}(\alpha_s^2) \right). \quad (\text{A.4})$$

We recall that charge conjugation implies $C_2^{\text{B1}}(Q^2, r) = -C_1^{\text{B1}}(Q^2, \bar{r})$, hence it suffices to discuss the case $i = 1$. A standard matching calculation of the $\gamma^* \rightarrow q\bar{q}g$ amplitude results in

$$\begin{aligned} \Delta^{\text{B1}}(Q^2, r) = & \left[\left(C_F - \frac{C_A}{2} \right) \left(-\frac{2}{\epsilon^2} + \frac{2}{\bar{r}\epsilon} + \frac{4r}{\bar{r}} + \frac{\pi^2}{6} \right) + C_F \frac{2}{\bar{r}} \right] \left(-\frac{\mu^2}{Q^2} \right)^{\epsilon} \\ & + \left[C_F \left(\frac{2}{\epsilon^2} - \frac{2r}{\bar{r}\epsilon} - \frac{1+5r}{\bar{r}} - \frac{\pi^2}{6} \right) + C_A \left(-\frac{2}{\epsilon^2} + \frac{r}{\bar{r}\epsilon} + \frac{1+r}{\bar{r}} + \frac{\pi^2}{6} \right) \right] \left(-\frac{\mu^2}{rQ^2} \right)^{\epsilon} \\ & + \left[C_F \left(-\frac{5}{\epsilon} - 10 \right) + C_A \left(-\frac{1}{\epsilon^2} + \frac{1}{\epsilon} + \frac{\pi^2}{12} \right) \right] \left(-\frac{\mu^2}{\bar{r}Q^2} \right)^{\epsilon} + \mathcal{O}(\epsilon). \end{aligned} \quad (\text{A.5})$$

The limit $r \rightarrow 0$ is of particular interest, and results in

$$\Delta^{\text{B1}}(Q^2, r) \stackrel{r \rightarrow 0}{\simeq} C_F \Delta^{A0} \left(-\frac{\mu^2}{Q^2} \right)^\epsilon + (C_F - C_A) \left(\frac{2}{\epsilon^2} - 1 - \frac{\pi^2}{6} \right) \left(-\frac{\mu^2}{rQ^2} \right)^\epsilon + \mathcal{O}(\epsilon, r), \quad (\text{A.6})$$

which shows that the B1 coefficient depends on two scales, Q^2 and rQ^2 . We can identify

$$\Delta^{A0} = -\frac{2}{\epsilon^2} - \frac{3}{\epsilon} - 8 + \frac{\pi^2}{6} + \mathcal{O}(\epsilon) \quad (\text{A.7})$$

with the one-loop contribution to the leading-power hard matching coefficient C^{A0} :

$$C^{A0}(Q^2) = 1 + \frac{\alpha_s C_F}{4\pi} \Delta^{A0} \left(-\frac{\mu^2}{Q^2} \right)^\epsilon + \mathcal{O}(\alpha_s^2). \quad (\text{A.8})$$

Comparing to (4.1), we find

$$D^{\text{B1}}(p^2) = 1 + \frac{\alpha_s}{4\pi} (C_F - C_A) \left(\frac{2}{\epsilon^2} - 1 - \frac{\pi^2}{6} \right) \left(-\frac{\mu^2}{p^2} \right)^\epsilon + \mathcal{O}(\alpha_s^2). \quad (\text{A.9})$$

For completeness, we check that the $r \rightarrow 1$ limit of $\Delta^{\text{B1}}(Q^2, r)$ does not contain $1/\bar{r}$ terms:

$$\begin{aligned} \Delta^{\text{B1}}(Q^2, r) \stackrel{r \rightarrow 1}{\simeq} & \left[C_F \left(\frac{2}{\epsilon} - 1 \right) + C_A \left(-\frac{1}{\epsilon^2} - \frac{1}{\epsilon} + 2 + \frac{\pi^2}{12} \right) \right] \left(-\frac{\mu^2}{Q^2} \right)^\epsilon \\ & + \left[C_F \left(-\frac{5}{\epsilon} - 10 \right) + C_A \left(-\frac{1}{\epsilon^2} + \frac{1}{\epsilon} + \frac{\pi^2}{12} \right) \right] \left(-\frac{\mu^2}{\bar{r}Q^2} \right)^\epsilon + \mathcal{O}(\epsilon, \bar{r}). \end{aligned} \quad (\text{A.10})$$

A.2 Derivation of the evolution equation of the asymptotic refactorization coefficient D^{B1}

Our goal is to show that the RGE (4.6) for the matching coefficient $D^{\text{B1}}(rQ^2)$ can be derived from the standard evolution equation of the hard-matching coefficient $C_i^{\text{B1}}(Q^2, r)$ for generic value of r . We note that this finding is distinct from the case of B1 operators containing a quark and a gluon in the same collinear direction, where the soft-gluon limit needs to be treated separately from the endpoint-regular piece [49].

The renormalization of SCET operators of the B1 type has been studied in detail in [44, 45], except for the fermion-number zero case, to which the operators $J_i^{\text{B1},\mu}(r)$ in (A.1) belong. The anomalous dimension matrix is determined by computing the $\overline{\text{MS}}$ renormalization factors $Z_{ij}^{\mu\nu}(r, s) = \delta_{ij} g_\perp^{\mu\nu} \delta(r-s) + \delta Z_{ij}^{\mu\nu}(r, s)$ defined via

$$J_{i,\text{ren}}^{\text{B1},\mu}(r) = \int ds Z_{ij}^{\mu\nu}(r, s) J_{j,\text{bare}}^{\text{B1},\nu}(s). \quad (\text{A.11})$$

Following the lines of [44, 45], we find at one-loop order $\delta Z_{ij}^{\mu\nu}(r, s) = g_\perp^{\mu\nu} \delta Z_{ij}(r, s)$ with

$$\begin{aligned} \delta Z_{11}(r, s) = \delta Z_{22}(r, s) = & -\frac{\alpha_s}{2\pi} \delta(r-s) \left[\frac{C_A}{\epsilon^2} + \frac{C_A}{\epsilon} \ln \left(\frac{\mu^2}{-Q^2 - i\varepsilon} \right) - \frac{C_A}{2\epsilon} \ln(r\bar{r}) + \frac{3C_F}{2\epsilon} \right] \\ & + \frac{\gamma(r, s)}{\epsilon}, \end{aligned} \quad (\text{A.12})$$

$$\delta Z_{12}(r, s) = \delta Z_{21}(r, s) = \frac{\alpha_s}{2\pi} \Delta_F \frac{2T_F}{\epsilon} r\bar{r}, \quad (\text{A.13})$$

where

$$\gamma(r, s) = \frac{\alpha_s}{2\pi} \left\{ \left(\frac{C_A}{2} - C_F \right) \left[\frac{\bar{r}}{\bar{s}} \left(\left(\frac{\theta(r-s)}{r-s} \right)_+ + \theta(r-s) \right) + \frac{r}{s} \left(\left(\frac{\theta(s-r)}{s-r} \right)_+ + \theta(s-r) \right) \right] + 2\Delta_F T_F r \bar{r} \right\}. \quad (\text{A.14})$$

The momentum fractions have support in the interval $0 \leq r, s \leq 1$. Furthermore, $T_F = 1/2$, and $\Delta_F = 1$ (0) in the flavour-singlet (non-singlet) projection of the anti-collinear $\bar{\chi}\bar{c}\chi\bar{c}$ fields in $J_i^{\text{B1},\mu}$. The expression in square brackets defines a symmetric distribution, which applies to integration over test functions of r or s , with definition

$$\int dr f(r) [D(r-s)]_+ = \int dr D(r-s) (f(r) - f(s)), \quad (\text{A.15})$$

$$\int ds [D(r-s)]_+ g(s) = \int ds D(r-s) (g(s) - g(r)). \quad (\text{A.16})$$

The definition applies to any integration range, which is left unspecified here. In (A.14) the integrations are limited to $0 \leq r, s \leq 1$, but we will also consider the case $0 \leq r, s \leq \infty$ below.

The anomalous dimension can then be obtained as

$$\Gamma = \mathbf{Z} \frac{d}{d \ln \mu} \mathbf{Z}^{-1}, \quad (\text{A.17})$$

giving the RGEs

$$\frac{d}{d \ln \mu} C_j^{\text{B1}}(Q^2, s) = \int_0^1 dr C_i^{\text{B1}}(Q^2, r) \Gamma_{ij}(r, s). \quad (\text{A.18})$$

Here we already used that the current renormalization for the specific operators $J_i^{\text{B1},\mu}(r)$ considered here is diagonal in Lorentz indices, such that they can be dropped in the Wilson coefficients and anomalous dimension matrix.

We checked that convolving the tree-level coefficients $C_i^{\text{B1}}(Q^2, r)$ with $\delta Z_{ij}(r, s)$ agrees with the divergent part of the explicit one-loop result for $C_j^{\text{B1}}(Q^2, s)$ as given in the previous subsection for the flavour non-singlet projection, including both the contributions that are singular as well as those that are regular with respect to the dependence on s . This confirms the observation that the standard evolution equation for the B1 current can be used in this context, despite of the soft (anti-)quark singularity for $r \rightarrow 0$ ($\bar{r} \rightarrow 0$). In the following we are interested in extracting from the evolution equation the part that describes the renormalization of the endpoint-singular piece captured by D^{B1} .

The all-order identity $C_2^{\text{B1}}(Q^2, r) = -C_1^{\text{B1}}(Q^2, \bar{r})$ is consistent with the relations $\delta Z_{11}(r, s) = \delta Z_{22}(r, s) = \delta Z_{22}(\bar{r}, \bar{s})$ and $\delta Z_{12}(r, s) = \delta Z_{21}(r, s) = \delta Z_{21}(\bar{r}, \bar{s})$. Furthermore it can be checked that $\delta Z_{12}(r, s)$ does not contribute to the renormalization of $D^{\text{B1}}(rQ^2)$, due to the independence on s (see below). Therefore it is sufficient to consider $Z(r, s) \equiv \delta(r-s) + \delta Z_{11}(r, s)$ in the following.

The matching coefficient $C_1^{\text{B1}}(Q^2, r)$ for the problem at hand features a power-like endpoint singularity $\propto 1/r$ for $r \rightarrow 0$, that may be modulated by logarithmic corrections,

and is captured by the D^{B1} contribution in (4.1). In order to extract the renormalization factor for D^{B1} , we are interested in the convolution with $\Gamma_{11}(r, s)$ (or equivalently $Z(r, s)$ at order α_s). The result of the convolution can be split into an endpoint divergent piece $\propto 1/s$, and a regular part. The former describes the renormalization of D^{B1} , and the latter yields a mixing of D^{B1} into the endpoint-finite part of $C_1^{\text{B1}}(Q^2, r)$. Here we are interested only in the endpoint-singular contribution. In order to isolate it, we consider test functions that represent the most general possible dependence of the Wilson coefficient on the momentum fraction, and investigate the integral

$$\int dr \frac{f(r)}{r} Z(r, s) = \frac{F(s)}{s} + \text{endpoint-regular}. \tag{A.19}$$

Here $f(r)$ is an arbitrary test function defined for $r \geq 0$, that depends logarithmically on r , and represents the D^{B1} coefficient. For example, $f(r)$ could be given by some power of $\ln(r)$ or a more general polylogarithmic dependence. The right-hand side states that the result can be written as an endpoint-singular piece, with some function $F(s)$ that also depends logarithmically on s , and an endpoint-regular contribution. Below we show that this is indeed the case, and that $F(s)$ can be obtained via

$$F(s) = \int dr f(r) Z_{A_0A_0} \times Z_{D^{\text{B1}}D^{\text{B1}}}(r, s), \tag{A.20}$$

with a renormalization factor $Z_{D^{\text{B1}}D^{\text{B1}}}(r, s)$, and $Z_{A_0A_0}$ the renormalization constant for the leading-power coefficient $C^{A_0}(Q^2)$, being given at order α_s by

$$Z_{A_0A_0} = 1 - \frac{\alpha_s}{2\pi} \left[\frac{C_F}{\epsilon^2} + \frac{C_F}{\epsilon} \ln \left(\frac{\mu^2}{-Q^2 - i\epsilon} \right) + \frac{3C_F}{2\epsilon} \right]. \tag{A.21}$$

The strategy for obtaining $Z_{D^{\text{B1}}D^{\text{B1}}}$ is to apply the method of regions [50] to (A.19), and expanding the integrand such that a homogeneous scaling in the limit $r, s \rightarrow 0$ is obtained.

As a first step, we need to check whether the integral over r exists, despite the endpoint-singular factor $1/r$. This is trivially the case for the local contribution to $Z(r, s)$, and we therefore only need to check the piece containing $\gamma(r, s)$,

$$\begin{aligned} \int dr \frac{f(r)}{r} \gamma(r, s) &= \frac{\alpha_s}{2\pi} \left(\frac{C_A}{2} - C_F \right) \left[\int_s^1 dr \left(\frac{\bar{r} f(r) - f(s)}{r - s} + \frac{\bar{r} f(r)}{\bar{s} r} \right) \right. \\ &\quad \left. + \int_0^s dr \left(\frac{r f(r) - f(s)}{s - r} + \frac{r f(r)}{s r} \right) \right] + \frac{\alpha_s}{\pi} \Delta_F T_F \int_0^1 dr r \bar{r} \frac{f(r)}{r}. \end{aligned} \tag{A.22}$$

The integrals in the second line exist due to the explicit factor r in the second line of (A.14), that cancels the endpoint-singularity $1/r$. The first line has no endpoint singularity due to the lower integration boundary.

As the next step, we need to expand the integrand assuming a homogeneous scaling for $r, s \rightarrow 0$. The first integral in the second line of (A.22) has already a homogeneous scaling, and only the first term in the round bracket contributes to $F(s)/s$, while the second term yields an endpoint-regular contribution $\int_0^s dr f(r)/s$. In addition, the integral in the

“singlet” term proportional to Δ_F is independent of s and can therefore not contribute to $F(s)$ in (A.19).

Let us now turn to the first line of (A.22). Expanding in the region of small r, s allows us to replace $\bar{r}/\bar{s} \rightarrow 1$. Next, we see that the integral $\int_s^1 dr f(r)/r$ contributes only to the endpoint-finite part on the right-hand side of (A.19), and can therefore be dropped in the present discussion. However, the first term in the round bracket in the first line of (A.22) yields contributions that scale as $1/s$. To isolate them, we replace the upper integration boundary 1 by a Heaviside function $\theta(1-r)$ within the integrand. The method of regions instructs us to homogenize also the Heaviside function, corresponding to extending the upper integration boundary to $+\infty$. At this point, we use that the test function $f(r)$ depends logarithmically on r . It can therefore be extended over the interval $0 \leq r < \infty$, in accordance with the method-of-region expansion. However, this procedure is too naive, since it implies that the integral diverges for $r \rightarrow \infty$. This problem is linked to the observation that the respective integral yields contributions that are logarithmically enhanced as $\ln(s)/s$ for $s \rightarrow 0$. They can in turn be isolated by the rewriting

$$\int_s^1 dr \frac{f(r)/r - f(s)/s}{r-s} = \int_s^1 dr \frac{f(r) - f(s)}{r(r-s)} + \frac{f(s)}{s} \ln(s). \quad (\text{A.23})$$

After this rewriting we can extend the integration range of the remaining integral to $s \leq r < \infty$, yielding the desired homogeneous scaling.¹⁶

Note that the relation above could equivalently be written at the level of plus-distributions, but we prefer to keep the explicit form here in order to be clear about the treatment of the integration domain in the various steps.

Altogether, this implies the contributions that scale as $1/s$ up to logarithmic corrections have been isolated, and are given by

$$\int dr \frac{f(r)}{r} \gamma(r, s) \Big|_{\alpha \ln(s)/s} = \frac{\alpha_s}{2\pi} \left(\frac{C_A}{2} - C_F \right) \left[\int_s^\infty dr \left(\frac{f(r) - f(s)}{r(r-s)} \right) + \frac{f(s)}{s} \ln(s) + \int_0^s dr \left(\frac{f(r) - f(s)}{s(s-r)} \right) \right]. \quad (\text{A.24})$$

By comparing with (A.19) we can read off the renormalization coefficient of D^{B1} ,

$$Z_{D^{\text{B1}} D^{\text{B1}}}(r, s) = \frac{\alpha_s(C_F - C_A)}{2\pi} \delta(r-s) \left[\frac{1}{\epsilon^2} + \frac{1}{\epsilon} \ln \left(\frac{\mu^2}{-rQ^2 - i\varepsilon} \right) \right] + \frac{\hat{\gamma}(r, s)}{\epsilon}, \quad (\text{A.25})$$

where

$$\hat{\gamma}(r, s) = \frac{\alpha_s}{2\pi} \left(\frac{C_A}{2} - C_F \right) s \left[\frac{\theta(r-s)}{r(r-s)} + \frac{\theta(s-r)}{s(s-r)} \right]_+, \quad (\text{A.26})$$

¹⁶We note the similarity of this procedure to the extraction of the “asymptotic kernel” for the QED-generalized light-cone distribution amplitude of a light meson in [37], which involves a colour-singlet but electrically charged operator.

and the plus distributions are defined with respect to the interval $0 \leq r, s < \infty$ here. The anomalous dimension is, at order α_s , given by

$$\Gamma_{D^{\text{B1}}D^{\text{B1}}}(r, s) = -\frac{d}{d \ln \mu} Z_{D^{\text{B1}}D^{\text{B1}}}(r, s) = 2\epsilon Z_{D^{\text{B1}}D^{\text{B1}}}(r, s) - \frac{\partial Z_{D^{\text{B1}}D^{\text{B1}}}}{\partial \ln \mu}, \quad (\text{A.27})$$

which gives

$$\Gamma_{D^{\text{B1}}D^{\text{B1}}}(r, s) = \frac{\alpha_s(C_F - C_A)}{\pi} \delta(r - s) \ln \left(\frac{\mu^2}{-rQ^2 - i\epsilon} \right) + 2\hat{\gamma}(r, s). \quad (\text{A.28})$$

We can express the result equivalently in terms of ω and $\hat{\omega}$ using $s = \omega/Q, r = \hat{\omega}/Q$. This yields

$$\frac{d}{d \ln \mu} D^{\text{B1}}(\omega) = \int_0^\infty d\hat{\omega} \gamma_D(\hat{\omega}, \omega) D^{\text{B1}}(\hat{\omega}), \quad (\text{A.29})$$

with

$$\begin{aligned} \gamma_D(\hat{\omega}, \omega) &= \frac{\alpha_s(C_F - C_A)}{\pi} \delta(\omega - \hat{\omega}) \ln \left(\frac{\mu^2}{-\omega Q - i\epsilon} \right) \\ &+ \frac{\alpha_s}{\pi} \left(\frac{C_A}{2} - C_F \right) \omega \left[\frac{\theta(\hat{\omega} - \omega)}{\hat{\omega}(\hat{\omega} - \omega)} + \frac{\theta(\omega - \hat{\omega})}{\omega(\omega - \hat{\omega})} \right]_+. \end{aligned} \quad (\text{A.30})$$

This result is consistent with eq. (3.2) in [36] obtained by a different method, when rewriting $\hat{\omega} \rightarrow x\omega$ and $\omega Q \rightarrow p^2$ in terms of the variables x and p^2 used there, and accounting for the different convention of the order of arguments of γ_D in (A.29).

B Alternative version of the endpoint-finite factorization formula

In this appendix consider the alternative split of the integration regions mentioned in section 4.3, i.e. we present the factorization formula for the version (1), corresponding to ω and ω' smaller than an endpoint factorization parameter Λ (integral I_1), and the complement region I_2 , see figure 6.

Subtracting the complement region I_2 , the A-type term takes the form

$$\begin{aligned} \frac{1}{\sigma_0} \frac{d\tilde{\sigma}}{ds_R ds_L} \Big|_{\text{A-type}} &= \frac{2C_F}{Q} f(\epsilon) |C^{\text{A0}}(Q^2)|^2 \tilde{\mathcal{J}}_{\tilde{\epsilon}}^{(\tilde{q})}(s_R) \int d\omega d\omega' \\ &\times \left\{ \tilde{\mathcal{J}}_c(s_L, \omega, \omega') \tilde{S}_{\text{NLP}}(s_R, s_L, \omega, \omega') \right. \\ &\quad - [1 - \theta(\Lambda - \omega)\theta(\Lambda - \omega')] \left[\tilde{\mathcal{J}}_c(s_L, \omega, \omega') \right] \left[S_{\text{NLP}}(s_R, s_L, \omega, \omega') \right] \\ &\quad \left. + \tilde{\mathcal{J}}_c(s_L, \omega, \omega') \tilde{S}_{\text{NLP}}(s_R, s_L, \omega, \omega') \right\}. \end{aligned} \quad (\text{B.1})$$

If we further assume that $\Lambda \gg 1/s_R, 1/s_L$, then we can keep only the leading terms in $1/(s_R\Lambda)$ and $1/(s_L\Lambda)$ and the previous equation simplifies to

$$\begin{aligned} \frac{1}{\sigma_0} \frac{\widetilde{d\sigma}}{ds_R ds_L} \Big|_{\text{A-type}} &= \frac{2C_F}{Q} f(\epsilon) |C^{A0}(Q^2)|^2 \widetilde{\mathcal{J}}_{\bar{c}}^{(q)}(s_R) \int d\omega d\omega' \\ &\times \left\{ \theta(\Lambda - \omega)\theta(\Lambda - \omega') \left[\widetilde{\mathcal{J}}_c(s_L, \omega, \omega') \widetilde{S}_{\text{NLP}}(s_R, s_L, \omega, \omega') \right. \right. \\ &\quad \left. \left. + \widetilde{\mathcal{J}}_c(s_L, \omega, \omega') \widetilde{S}_{\text{NLP}}(s_R, s_L, \omega, \omega') \right] \right. \\ &\quad + [\theta(\omega - \Lambda)\theta(\Lambda - \omega') + \theta(\omega' - \Lambda)\theta(\Lambda - \omega)] \left[\widetilde{\mathcal{J}}_c(s_L, \omega, \omega') \widetilde{S}_{\text{NLP}}(s_R, s_L, \omega, \omega') \right. \\ &\quad \left. \left. - [\widetilde{\mathcal{J}}_c(s_L, \omega, \omega')] \llbracket S_{\text{NLP}}(s_R, s_L, \omega, \omega') \rrbracket + \widetilde{\mathcal{J}}_c(s_L, \omega, \omega') \widetilde{S}_{\text{NLP}}(s_R, s_L, \omega, \omega') \right] \right\}. \end{aligned} \quad (\text{B.2})$$

The remaining part I_1 of the scaleless integral (4.16) must be combined with the B-type term. To make notation more concise, we introduce $r_\Lambda \equiv \Lambda/Q$. The B-type term for $i = i' = 1$ is

$$\begin{aligned} \frac{1}{\sigma_0} \frac{\widetilde{d\sigma}}{ds_R ds_L} \Big|_{\text{B-type}} \Big|_{i=i'=1} &= \frac{2C_F}{Q^2} f(\epsilon) \mathcal{J}_c^{(g)}(s_L) S^{(g)}(s_R, s_L) \int_0^\infty dr dr' \\ &\times \left\{ \theta(1-r)\theta(1-r') C_1^{\text{B1}*}(Q^2, r') C_1^{\text{B1}}(Q^2, r) \mathcal{J}_{\bar{c}}^{q\bar{q}(8)}(s_R, r, r') \right. \\ &\quad \left. - [\theta(r_\Lambda - r)\theta(r_\Lambda - r')] \llbracket C_1^{\text{B1}*}(Q^2, r') \rrbracket_0 \llbracket C_1^{\text{B1}}(Q^2, r) \rrbracket_0 \llbracket \mathcal{J}_{\bar{c}}^{q\bar{q}(8)}(s_R, r, r') \rrbracket \right\}. \end{aligned} \quad (\text{B.3})$$

If we choose $r_\Lambda \ll 1$, then the B-type term simplifies to

$$\begin{aligned} \frac{1}{\sigma_0} \frac{\widetilde{d\sigma}}{ds_R ds_L} \Big|_{\text{B-type}} \Big|_{i=i'=1} &= \frac{2C_F}{Q^2} f(\epsilon) \mathcal{J}_c^{(g)}(s_L) S^{(g)}(s_R, s_L) \int_0^1 dr \int_0^1 dr' [1 - \theta(r_\Lambda - r)\theta(r_\Lambda - r')] \\ &\times \left\{ C_1^{\text{B1}*}(Q^2, r') C_1^{\text{B1}}(Q^2, r) \mathcal{J}_{\bar{c}}^{q\bar{q}(8)}(s_R, r, r') \right. \\ &\quad \left. - \llbracket C_1^{\text{B1}*}(Q^2, r') \rrbracket_0 \llbracket C_1^{\text{B1}}(Q^2, r) \rrbracket_0 \llbracket \mathcal{J}_{\bar{c}}^{q\bar{q}(8)}(s_R, r, r') \rrbracket \right\} \end{aligned} \quad (\text{B.4})$$

up to corrections of $\mathcal{O}(\Lambda/Q)$. Just as for version (2) given in the main text, we can obtain the $i = i' = 2$ case by $C_1^{\text{B1}(\ast)} \rightarrow C_2^{\text{B1}(\ast)}$, $\llbracket \dots \rrbracket_0 \rightarrow \llbracket \dots \rrbracket_1$ and $r^{(\prime)} \rightarrow \bar{r}^{(\prime)}$.

Open Access. This article is distributed under the terms of the Creative Commons Attribution License ([CC-BY 4.0](https://creativecommons.org/licenses/by/4.0/)), which permits any use, distribution and reproduction in any medium, provided the original author(s) and source are credited. SCOAP³ supports the goals of the International Year of Basic Sciences for Sustainable Development.

References

- [1] S. Catani, G. Turnock, B.R. Webber and L. Trentadue, *Thrust distribution in e^+e^- annihilation*, *Phys. Lett. B* **263** (1991) 491 [[INSPIRE](#)].
- [2] S. Catani, L. Trentadue, G. Turnock and B.R. Webber, *Resummation of large logarithms in e^+e^- event shape distributions*, *Nucl. Phys. B* **407** (1993) 3 [[INSPIRE](#)].

- [3] Y.L. Dokshitzer, D. Diakonov and S.I. Troian, *Hard semiinclusive processes in QCD*, *Phys. Lett. B* **78** (1978) 290 [INSPIRE].
- [4] G. Parisi and R. Petronzio, *Small transverse momentum distributions in hard processes*, *Nucl. Phys. B* **154** (1979) 427 [INSPIRE].
- [5] J.C. Collins and D.E. Soper, *Back-to-back jets in QCD*, *Nucl. Phys. B* **193** (1981) 381 [Erratum *ibid.* **213** (1983) 545] [INSPIRE].
- [6] J. Kodaira and L. Trentadue, *Can soft gluon effects be measured in electron-positron annihilation?*, *Prog. Theor. Phys.* **69** (1983) 693 [INSPIRE].
- [7] T. Becher and M.D. Schwartz, *A precise determination of α_s from LEP thrust data using effective field theory*, *JHEP* **07** (2008) 034 [arXiv:0803.0342] [INSPIRE].
- [8] D. Bonocore, E. Laenen, L. Magnea, L. Vernazza and C.D. White, *Non-Abelian factorisation for next-to-leading-power threshold logarithms*, *JHEP* **12** (2016) 121 [arXiv:1610.06842] [INSPIRE].
- [9] I. Moulton, I.W. Stewart, G. Vita and H.X. Zhu, *First subleading power resummation for event shapes*, *JHEP* **08** (2018) 013 [arXiv:1804.04665] [INSPIRE].
- [10] M. Beneke et al., *Leading-logarithmic threshold resummation of the Drell-Yan process at next-to-leading power*, *JHEP* **03** (2019) 043 [arXiv:1809.10631] [INSPIRE].
- [11] I. Moulton, I.W. Stewart and G. Vita, *Subleading power factorization with radiative functions*, *JHEP* **11** (2019) 153 [arXiv:1905.07411] [INSPIRE].
- [12] N. Bahjat-Abbas et al., *Diagrammatic resummation of leading-logarithmic threshold effects at next-to-leading power*, *JHEP* **11** (2019) 002 [arXiv:1905.13710] [INSPIRE].
- [13] M. Beneke, M. Garny, S. Jaskiewicz, R. Szafron, L. Vernazza and J. Wang, *Leading-logarithmic threshold resummation of Higgs production in gluon fusion at next-to-leading power*, *JHEP* **01** (2020) 094 [arXiv:1910.12685] [INSPIRE].
- [14] I. Moulton, I.W. Stewart, G. Vita and H.X. Zhu, *The soft quark Sudakov*, *JHEP* **05** (2020) 089 [arXiv:1910.14038] [INSPIRE].
- [15] M. Beneke, A. Broggio, S. Jaskiewicz and L. Vernazza, *Threshold factorization of the Drell-Yan process at next-to-leading power*, *JHEP* **07** (2020) 078 [arXiv:1912.01585] [INSPIRE].
- [16] I. Moulton, G. Vita and K. Yan, *Subleading power resummation of rapidity logarithms: the energy-energy correlator in $N = 4$ SYM*, *JHEP* **07** (2020) 005 [arXiv:1912.02188] [INSPIRE].
- [17] A.H. Ajjath, P. Mukherjee and V. Ravindran, *Next to soft corrections to Drell-Yan and Higgs boson productions*, *Phys. Rev. D* **105** (2022) 094035 [arXiv:2006.06726] [INSPIRE].
- [18] M. Beneke, M. Garny, S. Jaskiewicz, R. Szafron, L. Vernazza and J. Wang, *Large- x resummation of off-diagonal deep-inelastic parton scattering from d -dimensional refactorization*, *JHEP* **10** (2020) 196 [arXiv:2008.04943] [INSPIRE].
- [19] A.H. Ajjath, P. Mukherjee, V. Ravindran, A. Sankar and S. Tiwari, *On next to soft threshold corrections to DIS and SIA processes*, *JHEP* **04** (2021) 131 [arXiv:2007.12214] [INSPIRE].
- [20] M. van Beekveld, L. Vernazza and C.D. White, *Threshold resummation of new partonic channels at next-to-leading power*, *JHEP* **12** (2021) 087 [arXiv:2109.09752] [INSPIRE].

- [21] Z.L. Liu and M. Neubert, *Factorization at subleading power and endpoint-divergent convolutions in $h \rightarrow \gamma\gamma$ decay*, *JHEP* **04** (2020) 033 [[arXiv:1912.08818](#)] [[INSPIRE](#)].
- [22] Z.L. Liu, B. Mecaj, M. Neubert and X. Wang, *Factorization at subleading power and endpoint divergences in $h \rightarrow \gamma\gamma$ decay. Part II. Renormalization and scale evolution*, *JHEP* **01** (2021) 077 [[arXiv:2009.06779](#)] [[INSPIRE](#)].
- [23] S. Fleming, A.H. Hoang, S. Mantry and I.W. Stewart, *Jets from massive unstable particles: top-mass determination*, *Phys. Rev. D* **77** (2008) 074010 [[hep-ph/0703207](#)] [[INSPIRE](#)].
- [24] M.D. Schwartz, *Resummation and NLO matching of event shapes with effective field theory*, *Phys. Rev. D* **77** (2008) 014026 [[arXiv:0709.2709](#)] [[INSPIRE](#)].
- [25] C.W. Bauer, S.P. Fleming, C. Lee and G.F. Sterman, *Factorization of e^+e^- event shape distributions with hadronic final states in soft collinear effective theory*, *Phys. Rev. D* **78** (2008) 034027 [[arXiv:0801.4569](#)] [[INSPIRE](#)].
- [26] M. Beneke, A.P. Chapovsky, M. Diehl and T. Feldmann, *Soft collinear effective theory and heavy to light currents beyond leading power*, *Nucl. Phys. B* **643** (2002) 431 [[hep-ph/0206152](#)] [[INSPIRE](#)].
- [27] M. Beneke and T. Feldmann, *Multipole expanded soft collinear effective theory with non-Abelian gauge symmetry*, *Phys. Lett. B* **553** (2003) 267 [[hep-ph/0211358](#)] [[INSPIRE](#)].
- [28] C.W. Bauer, D. Pirjol and I.W. Stewart, *Soft collinear factorization in effective field theory*, *Phys. Rev. D* **65** (2002) 054022 [[hep-ph/0109045](#)] [[INSPIRE](#)].
- [29] T. Becher, M. Neubert and G. Xu, *Dynamical threshold enhancement and resummation in Drell-Yan production*, *JHEP* **07** (2008) 030 [[arXiv:0710.0680](#)] [[INSPIRE](#)].
- [30] R. Brüser, Z.L. Liu and M. Stahlhofen, *Three-loop quark jet function*, *Phys. Rev. Lett.* **121** (2018) 072003 [[arXiv:1804.09722](#)] [[INSPIRE](#)].
- [31] A. Broggio, S. Jaskiewicz and L. Vernazza, *Next-to-leading power two-loop soft functions for the Drell-Yan process at threshold*, *JHEP* **10** (2021) 061 [[arXiv:2107.07353](#)] [[INSPIRE](#)].
- [32] P. Banerjee, P.K. Dhani and V. Ravindran, *Gluon jet function at three loops in QCD*, *Phys. Rev. D* **98** (2018) 094016 [[arXiv:1805.02637](#)] [[INSPIRE](#)].
- [33] I. Moulton, L. Rothen, I.W. Stewart, F.J. Tackmann and H.X. Zhu, *Subleading power corrections for N -jettiness subtractions*, *Phys. Rev. D* **95** (2017) 074023 [[arXiv:1612.00450](#)] [[INSPIRE](#)].
- [34] M. Beneke and L. Vernazza, *$B \rightarrow \chi_{cJ}K$ decays revisited*, *Nucl. Phys. B* **811** (2009) 155 [[arXiv:0810.3575](#)] [[INSPIRE](#)].
- [35] A. Vogt, *Leading logarithmic large- x resummation of off-diagonal splitting functions and coefficient functions*, *Phys. Lett. B* **691** (2010) 77 [[arXiv:1005.1606](#)] [[INSPIRE](#)].
- [36] Z.L. Liu, M. Neubert, M. Schnubel and X. Wang, *Radiative quark jet function with an external gluon*, *JHEP* **02** (2022) 075 [[arXiv:2112.00018](#)] [[INSPIRE](#)].
- [37] M. Beneke, P. Böer, J.-N. Toelstede and K.K. Vos, *Light-cone distribution amplitudes of light mesons with QED effects*, *JHEP* **11** (2021) 059 [[arXiv:2108.05589](#)] [[INSPIRE](#)].
- [38] S.W. Bosch, R.J. Hill, B.O. Lange and M. Neubert, *Factorization and Sudakov resummation in leptonic radiative B decay*, *Phys. Rev. D* **67** (2003) 094014 [[hep-ph/0301123](#)] [[INSPIRE](#)].
- [39] Z.L. Liu and M. Neubert, *Two-loop radiative jet function for exclusive B -meson and Higgs decays*, *JHEP* **06** (2020) 060 [[arXiv:2003.03393](#)] [[INSPIRE](#)].

- [40] G.T. Bodwin, J.-H. Ee, J. Lee and X.-P. Wang, *Renormalization of the radiative jet function*, *Phys. Rev. D* **104** (2021) 116025 [[arXiv:2107.07941](#)] [[INSPIRE](#)].
- [41] T. Becher, M. Neubert and B.D. Pecjak, *Factorization and momentum-space resummation in deep-inelastic scattering*, *JHEP* **01** (2007) 076 [[hep-ph/0607228](#)] [[INSPIRE](#)].
- [42] M. Neubert, *Renormalization-group improved calculation of the $B \rightarrow X_s \gamma$ branching ratio*, *Eur. Phys. J. C* **40** (2005) 165 [[hep-ph/0408179](#)] [[INSPIRE](#)].
- [43] T. Becher and M.D. Schwartz, *Direct photon production with effective field theory*, *JHEP* **02** (2010) 040 [[arXiv:0911.0681](#)] [[INSPIRE](#)].
- [44] M. Beneke, M. Garny, R. Szafron and J. Wang, *Anomalous dimension of subleading-power N -jet operators*, *JHEP* **03** (2018) 001 [[arXiv:1712.04416](#)] [[INSPIRE](#)].
- [45] M. Beneke, M. Garny, R. Szafron and J. Wang, *Anomalous dimension of subleading-power N -jet operators. Part II*, *JHEP* **11** (2018) 112 [[arXiv:1808.04742](#)] [[INSPIRE](#)].
- [46] C.F. Berger, C. Marcantonini, I.W. Stewart, F.J. Tackmann and W.J. Waalewijn, *Higgs production with a central jet veto at NNLL+NNLO*, *JHEP* **04** (2011) 092 [[arXiv:1012.4480](#)] [[INSPIRE](#)].
- [47] S. Catani, M.L. Mangano, P. Nason and L. Trentadue, *The resummation of soft gluons in hadronic collisions*, *Nucl. Phys. B* **478** (1996) 273 [[hep-ph/9604351](#)] [[INSPIRE](#)].
- [48] D. Binosi, J. Collins, C. Kaufhold and L. Theussl, *JaxoDraw: a graphical user interface for drawing Feynman diagrams. Version 2.0 release notes*, *Comput. Phys. Commun.* **180** (2009) 1709 [[arXiv:0811.4113](#)] [[INSPIRE](#)].
- [49] M. Beneke, M. Garny, R. Szafron and J. Wang, *Violation of the Kluberg-Stern-Zuber theorem in SCET*, *JHEP* **09** (2019) 101 [[arXiv:1907.05463](#)] [[INSPIRE](#)].
- [50] M. Beneke and V.A. Smirnov, *Asymptotic expansion of Feynman integrals near threshold*, *Nucl. Phys. B* **522** (1998) 321 [[hep-ph/9711391](#)] [[INSPIRE](#)].